

***IN-VITRO AND IN-VIVO PERFORMANCE
ANALYSIS OF NITINOL AS ORTHOPEDIC
IMPLANTS***

Thesis Submitted

By

Sarmita Sinha

Doctor of Philosophy (Engineering)

**DEPARTMENT OF MECHANICAL ENGINEERING
FACULTY COUNCIL OF ENGINEERING & TECHNOLOGY
JADAVPUR UNIVERSITY
KOLKATA, INDIA
2019**

IN-VITRO AND IN-VIVO PERFORMANCE ANALYSIS OF NITINOL AS ORTHOPEDIC IMPLANTS

Submitted by

Sarmita Sinha

Under guidance of

Dr. Abhijit Chanda

Professor

Department of Mechanical Engineering

Jadavpur University, Kolkata- 700032

&

Dr. Samit Kumar Nandi

Professor

Department of Veterinary Surgery & Radiology

West Bengal University of Animal and Fishery Science, Kolkata-700037

&

Dr. Indranil Banerjee

Assistant Professor

Department of Biotechnology and Medical Engineering

National Institute of Technology, Rourkela, Orissa- 769008

Department of Mechanical Engineering

Jadavpur University

Kolkata -700032

**JADAVPUR UNIVERSITY
KOLKATA-700032, INDIA**

INDEX NO. 129/15/E

1. Title of the thesis:

“IN-VITRO AND IN-VIVO PERFORMANCE ANALYSIS OF NITINOL AS ORTHOPEDIC IMPLANTS”

2. Name, Designation & Institution of Supervisor/s:

Dr. Abhijit Chanda

Professor

Department of Mechanical Engineering

Jadavpur University

Kolkata-700032

&

Dr. Samit Kumar Nandi

Professor

Department of Veterinary Surgery & Radiology

West Bengal University of Animal and Fishery Science

Kolkata-700037

&

Dr. Indranil Banerjee

Assistant Professor

Department of Biotechnology and Medical Engineering

National Institute of Technology, Rourkela, Orissa- 769008

CERTIFICATE FROM THE SUPERVISOR/S

This is to certify that the thesis entitled “**In-Vitro And In-Vivo Performance Analysis Of Nitinol As Orthopedic Implants**” submitted by Sarmita Sinha, who got her name registered on 28/07/2015 for the award of **Ph.D.(Engineering) degree** of **Jadavpur University**, is absolutely based upon her ownwork under the supervision of **Dr. Abhijit Chanda,Dr. Samit Kumar Nandi and Dr. Indranil Banerjere**, and that neither her thesis nor any part of the same has been submitted for any degree / diploma or any other academic award anywhere before.

Dr. Abhijit Chanda

Professor
Department of Mechanical Engineering
Jadavpur University
Kolkata-700032

Dr. Samit Kumar Nandi

Professor
Department of Veterinary Surgery
& Radiology, West Bengal
University of Animal and Fishery
Science, Kolkata-700037

Dr. Indranil Banerjee

Assistant professor,
Department of Biotechnology and
Medical Engineering, NIT
Rourkela, Orissa- 769008

DEDICATION

*"To my Parents, Didi and my supervisor Dr.
Abhijit Chandra"*



PREFACE

This thesis is the result of my own work and includes nothing which is the outcome of work done in collaboration, except where specifically indicated in the text and acknowledgements. The research was conducted primarily at the Department of Mechanical engineering, Jadavpur University, School of Bio-Science and Engineering, Jadavpur University and also at the laboratories of West Bengal university of animal and Fishery Science, Kolkata, during the years from 2015 to 2019, under the supervision of Dr. Abhijit Chanda of Dept. of Mechanical Engineering, Jadavpur University, Dr. Samit Kumar Nandi, Department of Veterinary Surgery & Radiology, West Bengal University of Animal and Fishery Science, Kolkata and Dr. Indranil Banerjee, Department of Biotechnology and Medical engineering, NIT Rourkela

No part of this thesis has already been or is being concurrently submitted for any degree, diploma or other qualification.

ACKNOWLEDGEMENT

I would like to express my deepest appreciation to all those who helped me in their own ways for the completion of this thesis work. Time flies, of course it does. It seems my thesis work period just came to an abrupt end in no time at all. Through it all, I would like to express my gratitude to the most important person Dr. Abhijit Chanda, Dept. of Mechanical Engineering, Jadavpur University, whose constant support, esteemed guidance, invaluable suggestions, innovative ideas and affection at every stage of my work and life have steered me through to the end of my work. I find immense pleasure to have had him as my thesis advisor. He has not only been my guide but more like a friend, a fatherly figure to me. Without him conceiving this study would have been impossible. My heart will always bear respectful gratitude to him. A mere 'Thank you' would fall far short to express my heartfelt regards to the very person I owe a ton to.

My deepest gratitude goes to my co-guides Dr. Samit Kumar Nandi, Department of Veterinary Surgery & Radiology, West Bengal University of Animal & Fishery Science, Kolkata and Dr, Indranil Banerjee, Assistant professor, Department of biotechnology and Medical Engineering. I am very grateful for their tremendous help and kind support behind this research. They educated me on different aspects of animal trials and cell culture study. The thesis work would never be possible without their help.

I gratefully acknowledge the funding authority Council for Scientific & Industrial Research for their financial support(file no 09/096(0803)/2014-EMR-1)

I express my gratefulness to Director, Piyali Basak and all faculties and staff members of School of Bio Science & Engineering, Jadavpur University, Kolkata.

I would like to thank Honourable Vice Chancellor, West Bengal University of Animal and Fishery Sciences for providing me the facilities to do this research work .

I like to express my special gratitude to HOD, faculties and staffs of Mechanical Engineering Department for giving me opportunities to go with this work.

I am especially grateful to Dr. Jerzy Kubacki, A. Chelkowski Institute of Physics, University of Silesia, Katowice, Poland for the experimental support I received from him without which one of my modification technique was not possible.

I convey my heartfelt thanks to Sidhartha Patra Sir, Mechanical Engineering Department, Jadavpur University for his kind help.

I would like to thank S.P. Ghoshal Sir and Late Robiul Haque Sir who continuously inspired and motivated me and let my way to research.

I offer my cordial thanks to Dr. Biswanath Kundu, Dr. Dipten Bhattacharya and Tania, CGCRI, Kolkata, Rakibul Sir and Gafur Sir, BCSIR, Dhaka, Dr. Mangal Roy and K. Bavya Devi, Department of Metallurgical and Materials Engineering, IIT, Kharagpur, Dr. Soumen Das and Jyotsna Priyadarshini, SMST, IIT Kharagpur, Dr. Senthilguru Kulanthaivel, Sharan, Krishna, Yamini, Biotechnology and Biomedical Engineering Department, NIT Rourkela, Dr. Rajib Dey and Amit Kumar Bhandar, Pritha Pal, Sourav Adhikary, Department of Metallurgical & Material Engineering, Jadavpur University and Piyali Das, West Bengal University of Animal & Fishery Science, Kolkata for extending their help in material characterization, in-vitro and in vivo studies.

I want to convey my heartiest gratitude to all my batch mates, my friends, seniors and juniors for their kind and invaluable cooperation. My time at Jadavpur University was made enjoyable in large part due to them. I am grateful for time spent with them and our memorable trips to mountains. I would like to acknowledge KanchanDa, SujanDa, PrabirDa, PallabDa, KritikaDi, PromitaDi, SatarupaDi, SusmitaDi, PriyambadaDi, AnjaliDi, PriyankaDi and especially HowaDi who imparted immense love, help and constant support and also my friends Somali, Kristi, Neha, Sayanti, Anup, Asif, Soma, Ankit, Rupsa, Ishita. These beautiful souls literally made me feel at home. They have been a very important source of support, help and love. It was an immense pleasure to have had the opportunity to have worked with them.

I would also like to acknowledge Pranabesh, Ayatree, Debanjan for being more like a family member than juniors to me during my entire research work.

I want to convey my heartiest regards to Tiyasha, Satarupa, Swarnima who have been the close person to me not only during my research but also during all the times of thick and thin.

Last but certainly not the least, I owe much to my parents, my elder sister (Didi), Pipi, Rini and to all my family members and my extended family Soma maam, Akash, Batash, Anirban Sir would like to thank them from the bottom of my heart for their constant support, help, unconditional love and care without which no one of it would have been possible. Without their guidance I could have never achieved anything in any sphere of life.

March, 2019

Sarmita Sinha

Abstract

Nitinol is a very promising biomaterial to be used in medical treatment like surgical implants due to its unique properties. Nitinol has superelasticity, shape memory effect, kink resistance, good biocompatibility, biomechanical properties, corrosion resistance etc. Because of these properties Nitinol is a popular orthopedic implant material, but there is still need of surface modification of nitinol to control nickel leaching. It is a known fact that nickel is harmful for human body. Main challenge with such surface modification of orthopaedic implant is that along with cost effective modification of the surface, there should also be good integration with the surrounding bone tissue. The purpose of this study is to modify the nitinol surface by the silanization technique and electrophoretically deposited hydroxyapatite coating on nitinol surface and conduct a detail in-vitro and in-vivo investigation. X-ray photoelectron spectroscopy and energy dispersive X-ray spectroscopy studies confirmed the addition of organo-functional alkoxy silane molecules through the silanization process. From detailed investigations, involving MTT assay with the human osteoblastic cells (MG63 cell) over periods of 48 hours and 5 days and immunocytochemistry, it was found that silanized Nitinol performed marginally better than bare Nitinol. But in case of confocal image study, coated sample showed little bit better than silanized sample and bare sample respectively. The effect of silanization on surface composition and roughness of the specimen is also reported here to explain the superiority of silanized samples in case of cell-material interaction. A detailed animal study was also conducted for one and three months post operatively. The histological study showed the presence of adequate number of osteoblasts in silanized Nitinol and coated Nitinol. The fluorochrome labelling study depicted slightly better new bone formation in coated nitinol sample than silanized nitinol specimens and much better than bare one at one and three months postoperatively. Radiology and SEM study proved the better performance of silanized samples. The cumulative in-vitro and in vivo results indicate that coated and silanized nitinol samples are more or less showing same level of performance with silanized samples slightly better than the other. However both are suitable as the potential bio-implant materials in various orthopaedic surgical uses.

TABLE OF CONTENTS

Preface	vi
Acknowledgement	vii-ix
Abstract	x
List of tables	xii
List of figures	xiii-xv
List of Abbreviations	xvi-xvii
List of publication	xviii
Introduction	1-9
Literature survey	10-35
Objective	36-37
Materials and method	38-49
Results and discussion	50-75
Conclusion & Future scope	76-78

List of tables

Sl. No.	NAME OF THE TABLE	PAGE NO
Table 1.1	Three different generations of biomaterials are marked	1-2
Table 1.2	Biomedical uses of Nitinol based on its properties	5
Table 2.1	Few works on surface modification of Nitinol	19-20
Table 2.2	Few works on biofunctionalization of various biomaterials	22
Table 3.1	Sample type	45
Table 3.2	Animal group type:	45
Table 5.1	Lattice parameter of calcined pure and doped HAp powder	52
Table 5.2	Contact angle of (a)Bare Nitinol and (b) Silanized Nitinol	57
Table 5.3	Surface roughness of (a)Bare Nitinol and (b) Silanized Nitinol	58
Table 5.4	Comparison at a glance	73

List of Figures

Sl. No.	NAME OF THE FIGURE	PAGE NO
Figure 1.1	Implant material requirements	4
Figure 2.1	Basic crystal structure of austenitic Nitinol alloy	10
Figure 2.2	The martensite-austenite transformation. MS = martensite start temperature, Mf = martensite finish temperature, AS = austenite start temperature, Af = austenite finish temperature, H = hysteresis	12
Figure 2.3	Diagrammatic representation of the super-elasticity effect of NiTi alloy	13
Figure 2.4	The stress-strain curves of some biological materials are superimposed on those of stainless steel and Nitinol.	15
Figure 2.5	Various uses of Nitinol in Biomedical Application	16
Figure 3.1	Flow chart of HAp powder preparation	40
Figure 3.2	Electrophoretic deposition technique	41
Figure 3.3	Surgery technique(a) Bone defect area (b)bone defect (c) implant placed in the bone defect (d) after stitching	46
Figure 5.1a	FESEM and EDAX of Bare NiTi	50
Figure 5.1b	FESEM and EDAX of Silanized NiTi	50
Figure 5.2	(a) XPS of bare nitinol; (b) XPS of silanized nitinol; (c) Si2p spectra from the silanized sample.	51
Figure 5.3	XRD of Pure HAp	52
Figure 5.4	FTIR of Pure HAp	53
Figure 5.5a	FESEM of HAp Coated NiTi	53
Figure 5.5b	EDAX of HAp Coated NiTi	54
Figure 5.6	XRD of HAp powder scratched from the Coated NiTi	55

Figure 5.7	Ni+ leaching study over seven days	56
Figure 5.8	Contact angle of a) Bare Nitinol b) Silanized Nitinol c) Coated Nitinol	56
Figure 5.9	Surface roughness (A)2D profile of Bare Nitinol (B) 3D profile of Bare Nitinol (C)2D profile of Silanized Nitinol (D) 3D profile of Silanized Nitinol	57
Figure 5.10	Phase contrast micrographs A) Control NiTi, B)BareNiTi, C) SilanizedNiTi	59
Figure 5.11	Cell count data of bare nitinol and silanized nitinol (48hours) (n=5)	59
Figure 5.12	Cell proliferation (48 hours) (n=3)	60
Figure 5.13	Fluorescence micrographs: Here blue corresponds to (DAPI) and red (TRITC Phalloidin) corresponds to the nucleus and F-actin (a)Control (b)Bare NiTi (c)Silanized NiTi	60
Figure 5.14	MTT assay analysis of control, bare nitinol, silanized nitinol and HAp coated nitinol	61
Figure 5.15	2D and 3D Confocal micrographs of bare nitinol, silanized nitinol and coated nitinol samples	62
Figure 5.16	Hematoxylin and eosin (HE) stained histological images of Control sample section after one month, Bare Nitinol sample section after one month, Silanized Nitinol sample section after one month and Coated Nitinol sample section after one month Control sample section after three months, Bare Nitinol sample section after three months, Silanized Nitinol sample section after three months and coated Nitinol samples after three months	63
Figure 5.17	Radiological images of Control sample, Bare Nitinol sample, Silanized Nitinol sample and Coated Nitinol sample on 30 th day and on 90 th day	65
Figure 5.18	Fluorochrome labeling image of Control sample after one month and three months, Bare Nitinol sample after one month and three months , silanized Nitinol sample after 1month and 3months,	67

	Coated Nitinol sample after 1month and 3months . Host / old bone (green portion) and new bone (yellow portion , shown in percentage as well)	
Figure 5.19	SEM micrographs of (a) Bare Nitinol sample of 30days (b) Silanized Nitinol of 30 days (c) Coated Nitinol sample of 30days (1 denotes Nitinol implant,2 denotes tissue 3 denotes tissue growth over the implant 4 denotes the shortened gap between the implant and bone tissue)	67
Figure 5.20	Radiographic 2D images of defect bone sites showing extent of healing after 1month and 3 month (Red arrow showing new bone growth around the implant; yellow arrow showing implant material)	69
Figure 5.21	Radiographic 3D images of defect bone sites showing extent of healing after 1month and 3 month (Red arrow showing new bone growth around the implant; yellow arrow showing implant material)	70

List of abbreviations

NiTi	Nitinol
ASTM	American Society for Testing and Materials
APTES	3-aminopropyl)triethoxy saline
HAp	Hydroxyapatite
BD	Bulk density
EPD	Electrophoretic deposition
EDAX	Energy dispersive X-ray analysis
XRD	X-Ray Diffraction
JCPDS	Joint Committee On Powder Diffraction Standards
XPS	X-ray photoelectron spectroscopy
FTIR	Fourier Transform Infrared Spectroscopy
SEM	Scanning Electron Microscope
FESEM	Field emission Scanning Electron Microscope
FWHM	Full width At haf Maximum
MTT ASSAY	3-(4,5-Dimethylthiazol-2-yl)-2,5-diphenyltetrazolium bromidefor
SBF	Simulated body fluid
PBS	Phosphate buffer solution
OD	Optical Density
OTC	Oxy-tetracycline dihydrate

RBC	Red blood corpuscles
Ca-P	Calcium Phosphate
HC	Haversian Canal
SD	Standard Deviation
1M	One Month
3M	Three Months
DMEM	Dulbecco's modified eagle media
FBS	Fetal Bovine Serum
CPI	cell proliferation index
TRITC	Tetramethyl rhodamineisothio cyanate
	Phalloidin
DAPI	4', 6-diamidino-2-phenylindole

Research papers published:

Journals:

1. Sinha, S., Begam, H., Kumar, V., Nandi, S., Kubacki, J., & Chanda, A. (2018). Improved performance of the functionalized nitinol as a prospective bone implant material. *Journal of Materials Research*,33(17), 2554-2564.
2. Patra S., Sinha S. and Chanda A. (2018),Development and Finite Element Implementation of a Simple Constitutive Model to Address Superelasticity and Hysteresis of Nitinol P. Sahoo and J. P. Davim (eds.), *Advances in Materials, Mechanical and Industrial Engineering, Lecture Notes on Multidisciplinary Industrial Engineering, Chapter 8*,171-185.

Submitted:

Sinha S., Priyadarshini J., Bavya Devi K., Chanda A., Das S., Roy M. (2019), In vivo performance analysis of silanized and coated nitinol wires in biological environment. *Research in Veterinary Science*.

List of patents: Nil

List of presentations in national/international conferences

1. Sinha S., Begam H., Nandi S. and Chanda A. (2018),Verifying the effect of silanized nitinol surface : An in-vitro study, accepted in *Materials Today Proceedings*, Elsevier Publications, IOP Science, Amrita University, Incomamma 2018, August 2018.

CHAPTER 1: INTRODUCTION

The term ‘Biomaterial’ can be defined in many ways. A “*Biomaterial*” is any material, natural or man-made, that comprises whole or part of a living structure or biomedical device which performs, augments, or replaces a natural function. [1,2]. A biomaterial is a nonviable material used in medical device, intended to interact with biological systems. [3]. A biomaterial is any substance that has been engineered to interact with biological systems for a medical purpose - either a therapeutic (treat, augment, repair or replace a tissue function of the body) or a diagnostic one. The study of biomaterials is called biomaterials science or biomaterial engineering. This is not at all new domain of science. The practice of using biomaterials in surgery started few thousand years ago with some primitive understanding of science but it developed very fast in last two centuries. Biomaterials science today is the combination of basics of medicine, biology, chemistry, tissue engineering and materials science. It is an interdisciplinary branch of science having existed for around half a century. It is an exciting field of science, having experienced steady and strong growth over its history with large monetary investment. Table 1.1 presents a list of biomaterials in use.

Table 1.1: Three different generations of biomaterials are marked

FIRST GENERATION BIOMATERIALS	SECOND GENERATION BIOMATERIALS	THIRD GENERATION BIOMATERIALS
Biologically inert/ nearly inert	Bioactive	Bioactive and Bioresorbable
<ul style="list-style-type: none"> ➤ Metal (Stainless steel, Cobalt, chromium based alloys) ➤ Ceramics (Al_2O_3, ZnO_2) ➤ Polymer (silicone rubber, acrylic resins) etc 	<ul style="list-style-type: none"> ➤ Metal coated with a bioactive ceramic or chemically modified metal surface ➤ Ceramics (Bioactive glass, glass–ceramics and calcium phosphates (CaPs)) ➤ Polymers (Biodegradable polymers of synthetic and natural origin such as polyglycolide (PGA), polylactide (PLA)) 	Materials which have temporary three-dimensional porous structures and which are also able to activate genes that stimulate regeneration of living tissue are under this type of biomaterials.

Metals are used as biomaterials due to their superb mechanical properties, ductility and thermal conductivity. Metals have been used often in the development of porous structures on titanium based alloys. This type of titanium alloys with unique properties (shape memory, superelasticity) form a different group of biomaterial, termed as new generation biomaterial. This type of material used for medical applications, largely for implants in orthopaedics, for dental implants, stents etc. Shape memory alloys are used in various applications ranging from medical implants, such as cardiovascular & endoscopic stents, orthopedic screws and wires, dental archwires, to the manufacture of automotive actuators, aircraft, and electronic components. There is another catch-word often used to address such materials which is 'smart material'.

Smart materials are those materials which are planned in such a way that have one or more properties that can be extensively changed in an accurate manner by external stimuli, like stress, temperature, moisture, pH, electric or magnetic fields. One of the Smart Material Alloy wire is called 'Nitinol', as it is composed of nickel and titanium. This ordinary looking yet special kind of wire can be folded to form complex shapes quite easily and it conducts electricity Compared to regular steel or even copper wire. It is very expensive. The smart alloy Nitinol (**N**ickel **T**itanium **N**aval **O**rdnance **L**aboratory), the "metal with a memory," is revolutionizing manufacturing, engineering, and medicine as countless products that "think" for themselves enter the marketplace. This was discovered in 1959 by William J. Buehler of the U.S. Naval Ordnance Laboratory, its subsequent development was done by Buehler and Frederick E. Wang. Industrial NiTi alloys are prepared by either a primary vacuum induction melting (VIM) followed by vacuum arc melting (VAR) or by a multiple VAR process. [4]

One of the unique property is that this nitinol wire has a memory. If it is folded to form a shape and then heated above 90°C it comes back to its original shape. The shape memory effect occurs when a material returns to, or "remembers," its original cold-forged shape after being heated to deformation. It is attributed to a temperature-dependent phase change conditions with applied stress and strain (stress-induced martensite) in the solid state which is known as a thermo-elastic martensitic transformation [5,6,7]. The shape memory effect arising out of this transformation makes Nitinol a prospective biomaterial. It finds wide applications as biomaterial both in endoprosthesis as well as external devices.

Nitinol has another excellent property which is super-elasticity. Within a particular temperature range, it can be elastically strained up to 8-10%, much more than any conventional alloy. Beyond this temperature, Nitinol deforms similar to usual metals and alloys [8]. This unique property of superelasticity is nicely exploited in case of stent deployment [9, 10].

Nitinol has other special characteristics, and those are Fatigue Resistant, Elastic deployment , Thermal deployment, Kink resistance, Constant unloading stresses, Biomechanical compatibility, Dynamic interference, Hysteresis, MR compatibility, Uniform plastic deformation, Biocompatibility.

In case of designing various devices and implants the use of Nitinol is advantageous due its better flexibility and kink resistance, even while bent around tortuous paths [11]. It can be attributed to the reversible structural changes associated with super elastic behavior.

Biocompatibility means the ability of material to perform with an appropriate host response in a specific application. When materials are introduced to the body it is important not only that the material does not damage the body, but also that the environment of the body does not damage the implant. Two main factors determine the biocompatibility of a material: the host reactions induced by the material and the degradation of the material in the body environment. Because of the possibility of nickel (Ni) and titanium (Ti) ions to dissolve due to corrosion, it is important to understand the effects of these components.

Similar to other conservative materials, the force applied by a super-elastic device is not determined by strain, it is determined by temperature. As body temperature is assumed to be considerably constant, in case of superelastic materials like Nitinol, one can plan a tool which can apply a constant stress over a varied range of shapes. This offers a unique advantage as it reduces the chance of local stress accumulation. Moreover, the similarity between stress-strain behavior of Nitinol with natural materials leads to more quick and proper healing times and less disturbance to host tissue. The first product is the orthodontic arch-wire which was made by using this property [12].

Stainless steel, titanium and other metals are very rigid (with high young's modulus) compared to biological materials. It causes stress shielding of tissues whenever these

materials are placed parallel to natural tissue and carry major share of load. The stress-strain diagram of these materials differ considerably from those of biological materials but Nitinol is an exception. Nitinol is mechanically similar to biological materials due to its amazing compliance. Even the stress–strain hysteresis which is closely associated with the reversible structural changes (Austenite to twinned Martensite and back) makes Nitinol similar to biological materials [13].

Nitinol is non-ferromagnetic alloy with a lower magnetic susceptibility than other metallic implant materials. MRI compatibility is associated to the susceptibility of a material relative to human tissue. For that MRI images of Nitinol are clear, crisp and with much less artifacts than other metallic implant materials [9].

High rate of work hardening of martensitic Nitinol results in uniform deformation, and it leads to lower peak stresses and strains which is an important necessity during designing of various biomedical instruments.

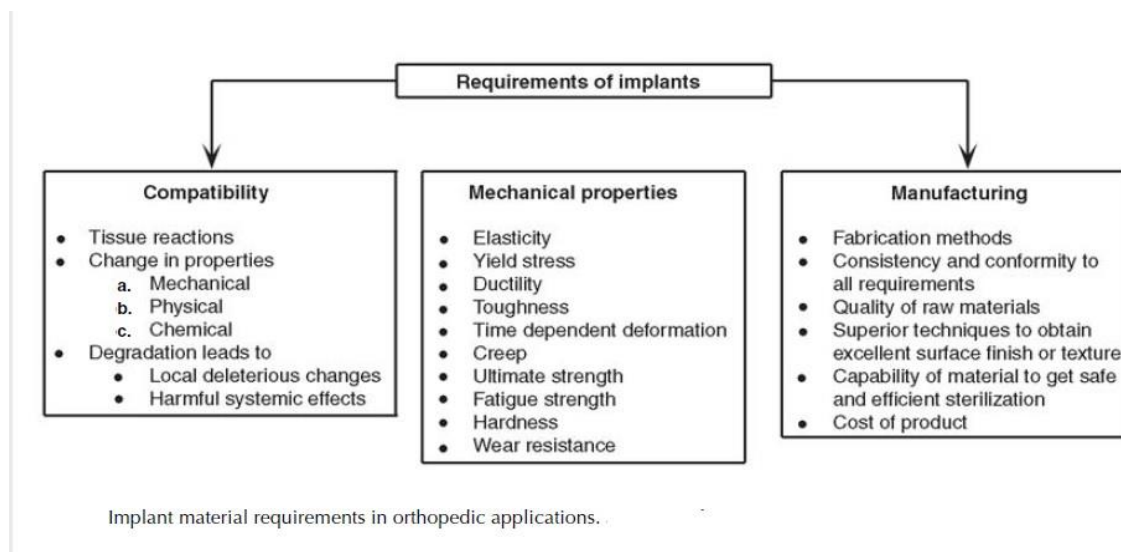


Figure 1.1: Implant material requirements

North America is the largest market for biomaterials owing to the refined healthcare infrastructure and amicable reimbursement policies in this region, followed by Europe. The global biomaterials market is assessed to reach \$139 Billion by 2022, growing at a CAGR of 11.8% from 2016 to 2022. Metal Biomaterials is estimated the largest of material types accounted for US\$33.7 billion in 2017 and is expected to reach US\$77 billion by 2023 at a CAGR of 14.7% between 2017 and 2023. Shape Memory Alloys Market worth reach 18.97 Billion USD by 2022. The shape memory alloys market is projected to reach USD

18.97Billion by 2022, at a CAGR of 12.3% from an estimated USD 10.62 Billion in 2017. The above mentioned figures make it amply clear that the biomaterials with exotic properties are going to find wide market in the years to come.

Apart from all these mentioned above, there are many more intricate areas where Nitinol based implants and appliances are being tried or are already in use.

Table 1.2: Biomedical uses of Nitinol based on its properties

Properties	Application
Shape memory effect	Bone plates, compression staples, nails, dental implants, vena cava filter, intracranial staples
Super elasticity	Stents
Elastic deployment	Homer mammalok, TUNA, RITA, ASDOS, Graspers, suture, passers, needle
Thermal deployment	Simon vena cava filter, stents
Biocompatibility	All Nitinol made implants
Kink resistance	Angioplasty guide wires, laproscopic instruments, IABP
Constant loading stresses	Spacer, Ω shape orthopaedic implant, orthodontic wire
Biomechanical compatibility	Dental implants
MR compatibility	All Nitinol made implants
Fatigue resistance	Dental drills, stents, pace-maker leads,
Uniform plastic deformation	Paragon stent. staple for female sterilisation, suture anchor, ACL prosthesis

1.1. Early Research and Uses of Nitinol: Progress in getting Nitinol into consumer applications came slowly because of early problems with its manufacture and because of its expense [14]. Another major problem was inconsistency among batches of Nitinol. Supposedly identical batches did not possess the same transition temperature. These inconsistencies were not a problem for laboratory demonstrations, but they hindered the manufacture of viable engineering materials. Buehler and Wang's research group at NOL continued to work on and refine the Nitinol manufacturing process until the bugs and glitches were eliminated [15,16].

The first successful Nitinol product was the Raychem Corporation's Cryofit™ "shrinkto-fit" pipe coupler, introduced in 1969 [17,18]. Another early use of Nitinol was in orthodontic bridge wires [19].

Though Nitinol has some unique properties but there are some drawbacks as well. One of the main constituents of Nitinol is nickel which is carcinogenic to human health beyond certain amount. Nickel, an essential element in the human body, should be present within a limit for daily digestion up to 200–300µg/day [20]. Due to corrosion, nickel ion may leach out from the surface and cross that dietary limit. Nickel ions can be released from the Nitinol alloy due to corrosion in biological atmosphere which is unavoidable [21]. Excessive Ni leaching in the body can cause many adverse effects like asthma, cytotoxicity, genotoxicityetc [22,23].

The method to tackle Ni⁺ leaching is surface modification of nitinol. There are various techniques to modify the surface, like laser treatment, coating, mechanical and chemical modification, biofunctionalization etc.

1.2. Surface modification: Surface modification of biomaterials is a significant way to modify the materials' responses to cells whilst retaining their bulk properties.

Nitinol is reported to maintain its corrosion resistance through formation of oxide layers. The oxide layer formation process is very slow and breakdown of this layer can occur in chloride containing atmosphere. The corrosion property and biocompatibility of Nitinol alloys largely depends the stability of this oxide layer thickness [24,25]. Major option exploited so far is to impart coating of various biomaterials. Many bioactive and bio-inert materials like hydroxyapatite, biphasic calcium phosphate, zirconia, diamond like carbon, polymers have been used for this purpose. Magneto-electropolishing (MEP) treatment, Plasma nano-coatings are the coating methods of surface modification that provided stable oxides on the surface and significantly improved the corrosion resistance and biocompatibility of the alloys [26].

In case of mechanical polishing, presence of residual stress and defective surface layers are reported to cause formation of cracks parallel to the surface. There may be additional factors like presence of grinding marks and scratching as well as chemical heterogeneity of the surfaces induced by mechanical polishing action. However, reports are available where mechanical and heat treatment increased biological activities. [27].

Surface modification using laser treatment is another process which includes surface alloying, cladding, annealing and transformation hardening of materials [28].

Biofunctionalization is a comparatively easy surface modification process which is readily accepted by the host organisms. Typically, proteins and peptides are adsorbed or coupled to biomaterials to alter cell phenotype or tissue response. Owing to higher strength to weight ratio and superior biocompatibility, stainless steel and titanium based implants like Nitinol are often subjected to this type of treatment to ensure better bonding with biological tissues.

Till date the main focus on nitinol was on stents or other related areas where blood compatibility and shape memory effect played the major important role. The present work is probably first of its kind focussing on the kink resistance behaviour of nitinol. The basic outline of the work includes a comprehensive study on physical and biological performance of bare and treated nitinol with specific emphasis on coating and biofunctionalization. Though the exact objectives and plan of work are presented in chapter three, here it is worth mentioning that the main target is to develop a systematic database to explore the possibility of using nitinol as orthopaedic nails.

References:

1. Raghavan, V. 2010, Materials Science and Engineering- A First Course, Fifth Edition, Eastern Economy Edition.
2. The Science and Design of Engineering Materials, Schaffer, et al. and Materials Science and Engineering; An Introduction, Callister.
3. George B. Kauffman, Isaac Mayo ,” The Story Of Nitinol: The Serendipitous Discovery Of The Memory Metal And Its Applications”, The C H E M I C A L Educator , Springer , ISSN: 1430 - 4171, Vol . 2.
4. Barras J.D.C, Myers A. K. Nitinol – Its Use in Vascular Surgery and Other Applications. European Journal of Vascular and Endovascular Surgery.2000; 564–569.
5. Morgan B.N. Medical shape memory alloy applications – the market and its products. Materials Science and Engineering.2004; 16-23Duerig T,Pelton A, Stockel D. An overview of Nitinol medical applications. Materials Science and Engineering A.1999; 149–160.
6. Palmaz J. Balloon-Expandable Intravascular Stent.American Journal of Radiology.1988; 1263–1269.
7. Sauli K. Biocompatibility and biomechanical aspects of Nitinol shape memory metal implants. ISBN 951-42-7123-8 ISSN 0355-3221. November 2003.
8. Drexel M, Selvaduray G, Pelton A. The Effects of Cold Work and Heat Treatment on the Properties of Nitinol Wire. Medical Device Materials IV: Proceedings from the Materials & Processes for Medical Devices Conference 2007, DOI: 10.1361/cp2007mpmd114 114.
9. Duerig T, Pelton A, Stockel D. An overview of Nitinol medical applications. Materials Science and Engineering A.1999; 149–160.
10. Thompson A.S. An overview of nickel–titanium alloys used in dentistry. International Endodontic Journal.2000; 297–310.
11. Fukuyo S, Duerig T, Melton K, Stockel D, Waguian C. Engineering Aspects of Shape Memory Alloys.Butterworth-Heinemann, Boston.1990; 470.
12. Stockel D. Minimally Invasive Therapy & Allied Technology.2000; 81-88.
13. Shabaloskya S. Applications Medicales des Materiaux Intelligents,.Montreal, Canada, 8 December 1995.
14. Hanson, A. A. Technology Review 1991, 94(4), 26.
15. Wang, F. E; Buehler, W. J.; Pickart, S. Japanese Journal of Applied physics, 1965, 36, 3232.

16. Wang, F. E.; DeSavage, B. F.; Buehler, W. *Japanese Journal of Applied physics*, 1968, 39, 2166.
17. Kurtz, J. *The New York Times*, 19 May 1991, Section F, p 7.
18. *The Economist* 1982, 785(7260), 94.
19. Galton, L. *Parade: The Sunday Newspaper Magazine*, 12 June 1977, p 11.
20. Barrett D.R., Bishara E.S., and Quinn J.: Biodegradation of orthodontic appliances. Part I. Biodegradation of nickel and chromium in vitro. *Am. Journal of Orthodontics and Dentofacial Orthopedics*, 103, 8 (1993).
21. Thierry B, Tabrizian M, Savadogo O, Yahia L. Effects of sterilization processes on NiTi alloy: surface characterization. *Journal Of Biomedical Materials Research*.2000;88–98.
22. Thierry B, Tabrizian M, Trepanier C, Savadogo O, Yahia L. Effect of surface treatment and sterilization processes on the corrosion behavior of NiTi shape memory alloy. *Journal Of Biomedical Materials Research*.2000; 685–93.
23. Bansiddhi A, Sargeant T, Stupp S, Dunand D. Porous NiTi for bone implants: A review ,*Acta Biomaterialia*. 2008 ; 773–782
24. Cempel M, Nikel G. Nickel: a review of its sources and environmental toxicology. *Polish Journal Of Environmental Studies*. 2006, 375–82.
25. Meng Q, Liu Y, Yang H, Shariat B, Nam T. Functionally graded NiTi strips prepared by laser surface anneal. *Acta Materialia*. 2012; 1658–1668
26. Gill P, Musaramthota V, Munroe N, Datye A, DuaR,Haider W, McGoron A, Rokicki R. Surface modification of Ni–Ti alloys for stent application after magnetoelectropolishing. *Materials Science and Engineering C*. 2015; 37–44.
27. Sevilla P, Martorell F, Libenson C, Planell J, Gil F. Laser welding of NiTi orthodontic archwires for selective force application. *Journal of Material Science: Materials in Medicine*. 2008; 525–529.
28. Pequegna A, Michael A, Wang J, Lian K, Zhou Y, Khan M. Surface characterizations of laser modified biomedical grade NiTi shape memory alloys. *Materials Science and Engineering C*.2015; 367–378.

CHAPTER 2:
LITERATURE SURVEY

An extensive literature survey has been carried out to know the progress of the vigorous work performed so far on the field of nitinol. Many research works have been performed in this field from the late 60's. Apart from the researches for the clinical purpose, the variety of work has been performed can be broadly classified into various groups: mechanical, compositional, physical, chemical, biological etc. With the advancements in technology, more and more researches are being done minutely to find out the relationship between these properties, their microstructure, and to understand its mechanism. Following are few of the studies and experiments done on nitinol by various researchers across the world which gave a new dimension to this field of study. The survey not only reviles different areas which are already taken care of for the better understanding of the subject, also helps to identify the important areas which need special attention.

Accidentally in 1959 “metal with a remembrance”, Nitinol was discovered by William J. Buehler [1] and Buehler and Wang subsequently developed it [2]. The best known Nitinol composition is about 55% by weight nickel and about 45% by weight titanium [3]. Figure 2.1 shows the cubic atomic structure of Nitinol which can “memorize” a predetermined shape and return to this shape under certain temperature conditions. This metallic alloy goes through a complex phase change which is known as martensite-austenite transformation [4].

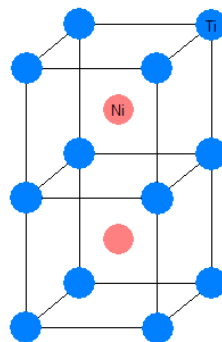


Figure 2.1: Basic crystal structure of austenitic Nitinol alloy

This case is the example of serendipity—the accidental happening which is a good feature that came out of a disastrous situation became a discovery only when the inventor realized its significance. In January 1958 William a metallurgist J. Buehler, at the Naval Ordnance Laboratory (NOL) had completed research on a series of iron–aluminium alloys [5] and suddenly came across this special variety of superelastic material [1].

Buehler consulted Max Hansen’s *Constitution of Binary Alloys* [6] which contained what was then the most complete collection of binary constitution diagrams, showing the solid-state phase relationships of two–component metallic alloys as a function of composition and

temperature. From approximately sixty intermetallic compound alloys Buehler selected twelve alloy systems [7] based on various logical reasons. One of the systems was an equiatomic nickel–titanium alloy, which immediately exhibited significantly more impact resistance and ductility than the other eleven alloys [8]. In 1953 Dr. Harold Margolin of New York University and his associates had carried out some studies on phase changes of nickel–titanium alloys but did not find any uniqueness among them [9]. In 1959 Buehler decided to focus on the equiatomic nickel–titanium composition alloys and relegate the intermetallic compound systems to secondary status. He named his finding NITINOL (Nickel Titanium Naval Ordnance Laboratory) [8]. That same year he made remark about his finding where he implied at the extraordinary, but still undiscovered, property of Nitinol [5].

In 1962 Dr. Frederick E. Wang joined Buehler’s group at the Naval Ordnance Laboratory, his expertise in crystal physics helped the discovery of how the shape memory property of Nitinol works. Without this the commercial applications of Nitinol would not have been possible [10]. An alloy such as Nitinol with a mechanical memory requires certain basic atomic structural characteristics. The first requisite is an atomically ordered solid-state parent phase, classically called austenite (named for the English metallurgist Sir William Chandler Roberts-Austen, 1843–1902) that exists in the higher temperature regime. Secondly, at a lower temperature, the atoms of the ordered austenite phase must be capable of solid-to-solid “shearing” into a very complex, new atomic arrangement or phase, which has been given the name martensite (named for the German metallographer, Adolf Martens, 1850–1914). The austenite martensite transformation (transition) proceeds through a critical temperature range or in special situations with applied stress and strain (stress-induced martensite). Thus Nitinol is said to undergo a martensite transformation.

Few key benefits of Nitinol are magnitude of strain-heat recovery, energy conversion, general corrosion resistance, human tissue and body fluid compatibility for medical applications, ease in reliably altering the memory-recovery temperature through alloying variations. With developed manufacturing techniques the commercial use of Nitinol increased during the 1970s and 1980s. Nitinol was incorporated into medical products, safety products, military products, and even ladies’ undergarments.

Some of the most important characteristic features of Nitinol and the research activities in those domains are presented below.

2.1. Shape memory effect: In case of Nitinol, shape-memory effect is one of the most vital characteristics. It is attributed to a temperature-dependent phase change conditions with applied stress and strain (stress-induced martensite) in the solid state which is known as a

thermo-elastic martensitic transformation [11, 12]. It requires basic atomic structural characteristics. First one is an atomically well-ordered solid-state parent phase, typically known as austenitic phase, prevalent at higher temperature. The other phase at lower temperature undergoes a shearing action to form a new atomic arrangement which is known as martensitic phase. Figure 2.2 demonstrate the phase transformation of Nitinol. The shape memory effect arising out of this transformation makes Nitinol a prospective biomaterial. It finds wide applications as biomaterial both in endoprosthesis as well as external devices.

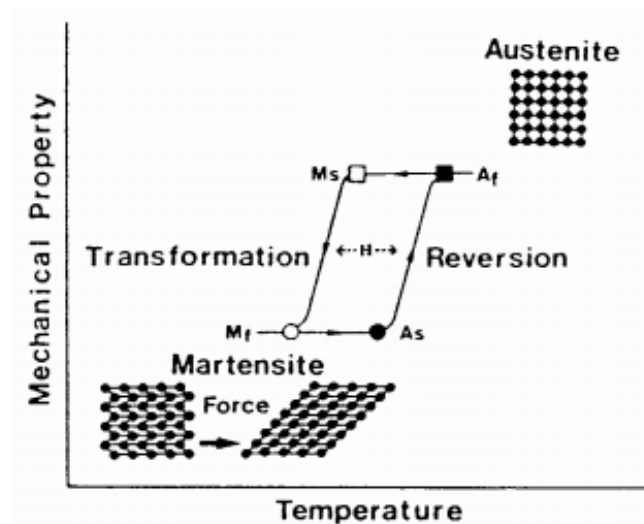


Figure 2.2: The martensite-austenite transformation. MS = martensite start temperature, Mf = martensite finish temperature, AS = austenite start temperature, Af = austenite finish temperature, H = hysteresis [4]

Allowing a constant and uniform constraint on different sections of broken bone, new bone plates are developed based on the shape memory effect [13-16]. In China, with the help of the shape memory effect, the removal of the staples from the bone were done by simple heating [11]. Another use of this property is in orthopedic nails for marrow cavity [18]. In the year of 1985, Fukuyo used Nitinol in dentistry to take the advantage of shape memory effect [19]. Another area of shape memory application of Nitinol is in stents. In vascular endo-surgery the use of Nitinol stents has become immensely popular in recent past [20-33]. Various designs of stents with Nitinol lattices covered with thin woven polyester showed consistently superior performance than conventional materials like stainless steel, tantalum etc. [34-36]. In 1971, Sawyer proposed fabrication of artificial heart with different sinusoidal elements to be made of Nitinol wires substituting the cardiac muscles [17]. Nitinol like shape memory alloys are reported to have adequate damping properties and are also being considered for hip

prosthesis [37]. Shape memory property was also exploited in Simon vena cave filter to get rid of large embolized blood clots in the vena cave vein [38].

2.2. Super elasticity: Nitinol can be elastically strained up to 8-10% which is much more than any conventional alloy within a particular temperature range. The usual range is well within 1% for most of the engineering metals and alloys. The super elastic property of Nitinol is based on stress-induced martensite formation and it is only possible up to a certain temperature range. Caused by externally applied forces, the highest temperature at which martensite can no longer be induced by stresses is called Martensite Deform Temperature (M_d). Beyond this temperature, Nitinol deforms similar to usual metals and alloys. On the lower end, the material is inherently martensitic below a specific temperature, known as the Austenite Start Temperature (A_s) where no super-elasticity prevails. Thus, from austenite finish (A_f) to martensite deform (M_d) temperatures the material is super-elastic [39]. This super-elasticity is nicely exploited in case of stent deployment. The encapsulated endovascular Nitinol stents are released from the chilled condition only when the catheter reaches the proper site and it starts to expand when the desired body temperature is attained. These stents can expand to 3–8 times the catheter diameter [40] provide a very low, dynamic outward force, yet a very high radial resistive force (RRF). Nitinol stents are often used for treating constricted hollow tubes such as the ureter, prostate, urethra, oesophagus or bile ducts [41-49]. It is also used as clips for intracranial aneurysms [50].

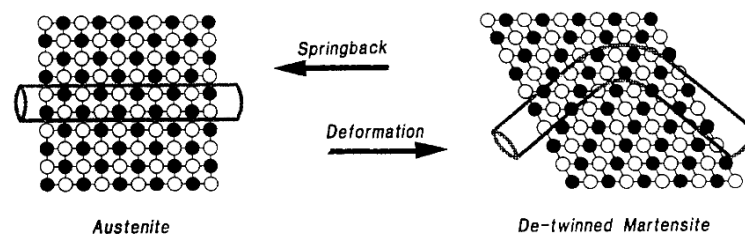


Figure 2.3: Diagrammatic representation of the super-elasticity effect of NiTi alloy [51]

Today complex operations are done by minor, leakage-proof portals into the body by passing wires and instruments percutaneously through needles into the various arteries and then elastically spring back into the desired shapes. To design these types of devices Nitinol gives the greatest liberty. Literature reveals that the first such product to be marketed was made of a Nitinol wire hook and a stainless steel cannulated needle [51], which was used to ‘mark’ the location of a breast tumour by the radiologists. Other devices are the transurethral needle ablation of the prostate (TUNA) device, the Daum deflectable puncture needle, and the

radiofrequency interstitial tissue ablation (RITA) device [52]. To make surgical instruments Nitinol can be worked into a shape that is suited for a particular procedure [51, 53]. Due to high resistance to rupture, super-elastic deformation etc Nitinol approaches the behaviour of a natural ligament [54,55]. The use of Nitinol for making artificial ligament is not yet fully achieved but it is an important application drawing attention of the researchers [56, 57].

Apart from shape memory effect and super-elasticity, other important characteristics which make Nitinol a highly prospective biomaterial are biocompatibility, kink resistance, biomechanical stability, MR compatibility.

2.3. Biocompatibility: The host reactions caused by the material and the deterioration of the material in the body environment are the two main features that determine the biocompatibility of a material. Nitinol forms a passive TiO_2 layer on the outer surface. The TiO_2 layer acts as the barrier for leakage of toxic nickel ions and also prevents corrosion in physiological environment [12]. Literature reveals that the formation of a passive titanium-oxide layer (TiO_2) is the main reason behind the very good biocompatibility of Ti alloys like Nitinol [58-62]. Formation of this layer is thermodynamically more favoured than other oxides [61-63]. Trepanier et al. reported the effects of surface engineering of Nitinol stents on their biocompatibility that revealed that electropolished and chemically passivated stents showed very high corrosion resistance due to the formation of thin and very uniform Ti-based oxide layer [59, 64-66]. In this context it may be mentioned that a slight discontinuity in the passivation layer (may be titanium oxide or calcium hydroxyapatite) can cause sustained leaching of nickel ion in biological fluid which in turn can affect biocompatibility.

2.4. Kink resistance: Nitinol is advantageous in case of designing various devices and implants due its better flexibility and kink resistance, even while bent around tortuous paths [67]. It can be attributed to the reversible structural changes associated with super elastic behavior. In conventional materials, permanent deformation in the shape of kink can form whenever local stresses due to some constriction exceeds yield point. But in Nitinol, elastic strain can go upto 8-10% and consequently the chance of kink formation is low. It reduces the scope of stress corrosion cracking as well. Thus angioplasty guide-wires of Nitinol coated with teflon or a hydrophilic coating in order to improve lubricity can easily pass through tortuous paths without kinking [68]. Another application of Nitinol is in super-elastic basket, for retrieval of stones from kidney, bladders, bile ducts [69].

2.5. Constant Loading Stresses: Applied force of a super-elastic device is determined by temperature. One can design a device with super-elastic Nitinol which can apply a continuous stress over a varied range of shapes as body temperature is assumed to be considerably constant. This offers a unique advantage as it reduces the chance of local stress accumulation. Additionally, the similarity between stress-strain behavior of Nitinol with natural materials leads to more quick and proper healing times and less disturbance to host tissue. The first product is the orthodontic arch-wire which was made by using this property [70]. There are different ranks of wire stiffness that permit the orthodontists to program the treatment stress to cause less pain [71-74]. Another application of this property is super-elastic eyeglass frames [75].

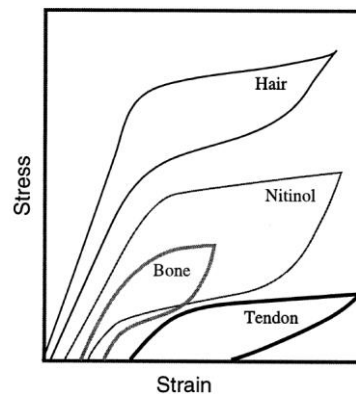


Figure 2.4: The stress-strain curves of some biological materials are superimposed on those of stainless steel and Nitinol. [40]

2.6. Biomechanical compatibility: Metals with high young's modulus are very rigid compared to biological materials. Due to this stress shielding of tissues happen whenever these materials are placed parallel to natural tissue and carry major share of load. The stress-strain diagram of these materials varies considerably from those of biological materials but Nitinol is an exception. Nitinol is mechanically comparable to biological materials due to its amazing compliance (Figure-2.4). Even the stress-strain hysteresis which is closely associated with the reversible structural changes (Austenite to twinned Martensite and back) makes Nitinol similar to biological materials [76]. Figure 2.4 explains the mechanical similarity of Nitinol with other biological materials like bone, tendon, and hair [40].

2.7. MR compatibility: As Nitinol is non-ferromagnetic alloy with a lower magnetic susceptibility than other metallic implant materials, for that MRI images of Nitinol are clear, crisp and with much less artifacts than other metallic implant materials [40]. It offers a

definite advantage over other conventional materials to understand the position and receptiveness of the implant to human tissue [5, 40].

2.8. Fatigue resistance: In high strain conditions, Nitinol offers exceptional fatigue resistance, while it may undergo fatigue in stress-controlled environments. Though the exact reason behind this differential response is not yet fully understood, primarily it can be attributed to higher capacity to undergo large elastic strain and a comparatively low value of yield stress. Classical extrusion-intrusion model of fatigue crack formation starts where local level yielding takes place. This might be one reason for higher susceptibility of Nitinol to stress controlled fatigue than strain controlled one. A recent application of Nitinol's excellent strain controlled fatigue property is in dental drills which is used for root canal procedures [40]. These drills can withstand severe fatigue environments. Another example of a strain-controlled application is pace-maker leads where requirement is a conductive metal without breaking which can survive very high numbers of flexing motions [40, 77-80]. In figure 2.5 various uses of Nitinol in biomedical field is described.

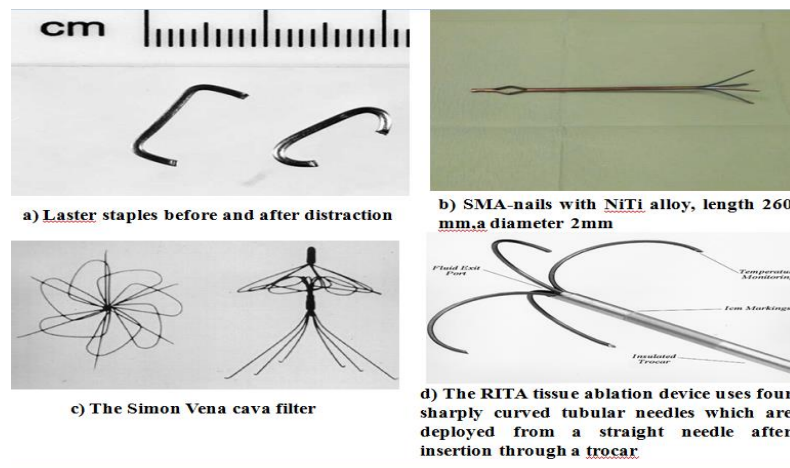


Figure 2.5: Various uses of Nitinol in Biomedical Application [81,82,38,40]

2.9. Uniform plastic deformation: Where high rate of work hardening of martensitic Nitinol results in uniform deformation, and it leads to lower peak stresses, Paragon balloon expandable stent is designed [40]. Typically shaped Nitinol staples are used for female sterilisation [84], internal fixation of fractures [50, 83]. Nitinol made Harrington rods are used for treating scoliosis using particular property.

Apart from all these mentioned above there are many more intricate areas where Nitinol based implants and appliances are being tried or are already in use [85-87]

2.10. Surface modification:

Surface modification is the action of modifying the surface of a material by physical, chemical or biological characteristics. [88-92]. Though Nitinol has some unique properties but there are some drawbacks as well. One of the main constituents of Nitinol is nickel which is carcinogenic to human health beyond certain amount. Due to corrosion, nickel ion may leach out from the surface and cross that dietary limit. Nickel ions can be released from the Nitinol alloy due to corrosion in biological atmosphere which is unavoidable [93]. Excessive Ni leaching in the body can cause many adverse effects like asthma, cytotoxicity, genotoxicityetc [93,94].

The oxide layer, which helps Nitinol to maintain its corrosion resistance forms very slowly and breakdown of this layer can occur in chloride containing atmosphere. The corrosion property and biocompatibility of Nitinol alloys largely depend on the stability of this oxide layer thickness [95-99]. There are other surface modification techniques as well to improve the surface property of Nitinol. They include mechanical treatments [100], electrochemical treatments, chemical etching, heat treatments, laser and electron-beam irradiation, coating etc. [101]. But almost all of these traditional methods have their own advantages as well as limitations. One problem which is almost common to all the above mentioned processes is the inconsistent corrosion behavior of the products. One major option exploited so far is to impart coating with various biomaterials. Many bioactive and bio-inert materials like hydroxyapatite, biphasic calcium phosphate, zirconia, diamond like carbon (DLC) have been used for this purpose [100, 102-105]. Calcium phosphate (hydroxyapatite) coating on Nitinol alloy improves the protection efficiency by 83% [103]. Diamond like carbon was also used by many researchers for surface modifications. Roy et al. used hybrid ion beam implantation technique for coating of DLC on Nitinol [106]. Sui et al. [107] used plasma immersion ion implantation and deposition technique to coat Nitinol using DLC and showed improvement in corrosion resistance and also surface hardness and elastic modulus. Corrosion resistance of Nitinol was improved by increasing the adhesion strength [108] of the coating with substrate. Polymers are also used for coating of Nitinol surface. Bakhshi et al used nanocomposite polymer derived from anti-thrombogenic and a non-biodegradable polymer, polyhedral oligo-mercisilsesquioxanes (POSS) and poly(carbonate-urea)urethane (PCU). This coating

enhanced the surface corrosion resistance property and improved the biocompatibility [109]. Magneto-electropolishing (MEP) treatment is another method of surface modification that provided stable oxides on the surface and significantly improved the corrosion resistance and biocompatibility of the alloys [110].

In case of mechanical polishing, presence of residual stress and defective surface layers are reported to cause formation of cracks parallel to the surface. There may be additional factors like presence of grinding marks and scratching as well as chemical heterogeneity of the surfaces induced by mechanical polishing action. However, reports are available where mechanical and heat treatment increased biological activities. Shen et al. showed improved cell adhesion by controlling the surface chemistry and surface hydrophilicity of Nitinol alloy [111]. They used mechanical treatment and chemical etching for controlling the surface roughness. Plasma nano-coatings significantly increased cell proliferation and cell adhesion on the micro patterned Nitinol surfaces [112].

Surface modification using laser treatment is another process which includes surface alloying, cladding, annealing and transformation hardening of materials. Generally fine laser light beam is used for surface modification and to perform localized treatment. Three types laser treatments are generally done in Nitinol manufacturing and surface modification. These are carbon dioxide laser, solid state laser (primarily neodymium:yttrium-aluminum-garnet; Nd:YAG laser) and excimer laser. Laser irradiation cause formation of nano/micro structure on Nitinol surface which changes the wettability and contact angle [113]. Laser melted surface are reported to improve the corrosion behavior of Nitinol. It causes the thickening of oxide layer, nitrogen incorporation and surface homogenization [114]. Pequeña et al [115] observed that ion release performance of Nd-YAG laser processed sample were worse compared to the other sample conditions (chemically etched and mechanical treated). It triggered some doubts regarding the suitability of the process. It has also been proposed that the performance of laser treated Nitinol can be improved by appropriate post processing treatments like mechanical polishing [116]. Laser annealing provoked intermixing of individual Ni and Ti layers which shows the formation of Nitinol inter-metallic compounds. Surface segregation of Ti and formation of TiO_2 are reported to improve biocompatibility [117]. Surface treated thin film Nitinol (S-TFN) is another potential material to cover the commercially used Nitinol stent through significant reduction in platelet adhesion without any evidence of aggregation [118]. Another option, alkali treatment on the Nitinol surface is

reported to increase the surface roughness, surface energy, wear resistance and hardness but it reduced the corrosion resistance and enhanced the nickel content [119]. Table 2.1 presents a summary of surface modification techniques applied on Nitinol in last two decades.

Table 2.1: Few works on surface modification of Nitinol

Surface modification	Technique	Outcome
Nd-YAG pulsed laser followed by Mechanical polishing [114]	Laser and mechanical treatment	Improved corrosion resistance and less nickel release
Coating of diamond like carbon (DLC) [107]	Plasma immersion ion implantation and deposition (PIIID)	Improvement in corrosion resistance and surface hardness and elastic modulus
Coating of Hap [104]	Sol-gel and electrochemically assisted deposition	Improvement in protection efficiency
Coating of diamond like carbon (DLC) [108]	hybrid magnetron sputtering and plasma enhanced chemical vapor deposition	better adhesion strength, the better corrosion resistance
Surface treatment [110]	Magneto-electropolishing	reduced the surface asperities on Nitinol alloys and provided stable oxides on the surface
Mechanical and chemical treatment [111]	Sandpaper grinding, chemical etching and Plasma nanocoating	Controllable surface roughness and hydrophilicity, improved cell adhesion
Coating [102]	ZrO ₂ coating	Improved corrosion resistance
Coating [118]	IrO ₂ coating	Better corrosion resistance
Mechanical, chemical, heat treatment	Etching with 1HF+4HNO, SiC paper	Chemical treatment

[119]	polishing , elctropolishing and heattreatment	showed consistent corrosion resistance, mechanical and heat treatment prone to pitting
Electroplating [120]	Electrodeposition of Tantalum in ionic liquid	Better corrosion resistance, higher open circuit potential, wider passive region and higher breakdown potential
Coating [112]	Silicon carbide coating	More than 90% reduction of Ni+ release, better anti-thrombogenicity
Coating [121]	Gelatin functionalized Grapheme oxide coating	Enhanced cell functions with antimicrobial activity
Bioactive coating [122]	Coating with poly(amino-p-xylylene-)	Decrease thrombogenicity, increased endothelialization, improved biocompatibility
Biofunctionalization[123]	Using polydopamine-immobilized rhBMP2	Enhanced bone tissue regeneration and osteointegration
Electrografting [124]	Modification of Nitinol by electrografting of 1,4-carboxybenzene diazonium	Better corrosion resistance

Although the traditional and advanced processes discussed above are often reported to yield good results in terms of increasing corrosion resistance of Nitinol, they offer certain inherent challenges as well. Stress induces deformation and crack formation, pitting, change in local

composition due to heating causing chemical heterogeneity are some of them. Also, there is ambiguity regarding the actual extent of betterment of biological performance achieved through these techniques. To address the above mentioned issues, in recent past, attempts have been made to explore the possibility of biological treatment like biofunctionalization which is discussed below.

2.11. Biofunctionalization: Biofunctionalization is a comparatively easy surface modification process which is readily accepted by the host organisms. Biofunctionalization is biologically compatible, permanent or temporary alteration of a material to have specific biological function. Various types of medical implants, tissue engineering scaffolds, cell culture platforms for cell expansion and in vitro assays, drug delivery systems, and imaging probes are designed to biofunctionalize to replace or repair a defective biological function so that they can be accepted by the host organism. Typically, proteins and peptides are adsorbed or coupled to biomaterials to alter cell phenotype or tissue response. Owing to higher strength to weight ratio and superior biocompatibility, stainless steel and titanium implants are often subjected to this type of treatment to ensure better bonding with biological tissues. In recent past, number of researchers have successfully done biofunctionalization of these materials. Table 2.2 summarises some of the important studies on biofunctionalization. These studies have involved various techniques of biofunctionalization on different types of metallic implants and judged the efficacy of those methods either through in-vitro or in-vivo studies. But till date only a few studies are available on the biofunctionalization of Nitinol. In 2016 Zhao et al have done gelatin-functionalized graphene oxide coating on Nitinol and found better antimicrobial activity and improved biocompatibility of Nitinol [135]. Simsek Yilmaz et al [136] coated Nitinol stents with star-PEG, and bio-functionalized with RGD, or RGD/CXCL1 and implanted into carotid arteries of mice. It has been reported that neointima formation and thrombus formation was substantially reduced and increased re-endothelialization [135] took place. In 2017, Karaji and his team have done additive manufacturing (selective laser melting) to develop multifunctional porous super-elastic Nitinol with a sensibly designed micro-architecture and biofunctionalized the surface using polydopamine-immobilized rhBMP2 for better control of the release kinetics [123]. They found improved cell attachment, cell proliferation, cell morphology (spreading, spindle-like shape), and cell coverage as well as elevated levels of ALP activity and increased calcium content for bio-functionalized surfaces as compared to as-manufactured specimens.

Table 2.2: Few works on biofunctionalization of various biomaterials

Material	Biofunctionalization agents	Purpose
Titanium [125]	polyelectrolyte multilayers (PEMs) of hyaluronic acid (HA) and chitosan (CH), coupled with surface-immobilized cell-adhesive arginine-glycine-aspartic acid (RGD) peptide	To improve the biocompatibility and confer long-lasting antibacterial properties on Ti made orthopaedic implants.
Titanium [126]	Grit-blasted and acid-etched dental implants coated with hydroxyapatite(HA) and then coated with a biomimetic active peptide(P-15)	To enhance attachment of the dental implant to the surrounding bone
Titanium [127]	Conjugating two strongest peptides with an integrin recognizing peptide motif, RGDS.	To measure the effect of peptide functionalization on bioactivity of Ti implant
Titanium [128]	cyclo (-RGDfK-) peptide	Development of an easy and practical coating for Ti implants
Titanium [129]	A mono-molecular adsorbed layer of a copolymer i.e., poly(Llysine)-graft-poly(ethylene glycol) (PLL-g-PEG) and its derivatives	To study the early bone apposition to a modified sandblasted and acid-etched (SLA) surface
Titanium and TiNbHf alloy [130]	Bioactive molecules, covalently coupled to the substrates	To study the influence of linear RGD, cyclic RGD, and recombinant fibronectin fragment III
Titanium [131]	Collagen grafting was done by either physisorption or covalent bonding.	To study the effect on human dermal fibroblast (HDF) cell response
Titanium [132]	covalently grafting two adhesive peptides on oxidized titanium substrates after silanization	To develop endosseous implant
Porus silicone	Chemical vapour deposition of 3-aminopropyltriethoxy silane (APTS) on its	To functionalize Porus Silicone surfaces for

(PS) [133]	surface.	biosensors
Stainless steel [134]	silane-coupling agent (SCA), (3-mercaptopropyl)trimethoxysilane	To prevent bovine serum albumin and γ -globulin adsorption which is helpful to design orthopedic implants

2.12. In-vivo studies of surface modified Nitinol: Any form of Nitinol whether as prepared or surface treated must be subjected to thorough and systematic animal trial before being considered as a commercial implant material. Takeshita et al. investigated the bone reaction to Nitinol and other materials inserted transcortically and extending into the medullary canal of rat tibiae [135]. Ni-Ti implants showed significantly lower percentage bone contact than any of the other titanium or titanium alloy materials. Trepanier et al studied quantification of the fibrous response of rabbit para-vertebral muscle in contact with Nitinol stents. Comparing with other materials they observed significantly higher fibro-cellular response around the heat treated Nitinol samples [136]. Thierry et al. [137] used laser cut Nitinol stents to replicate the configuration of stainless steel made Palmazs stents and tested in a porcine model under controlled conditions. They showed different thrombus morphologies for Nitinol and stainless steel along with the unique mechanical properties of Nitinol and haemocompatibility [137]. Kujala et al. [4] evaluated the effect of porosity on the osteointegration of Nitinol implants in rat bone. Muhonen et al. investigated bone response to sol-gel-derived titania-silica coated functional intramedullary Nitinol nails that applied a continuous bending force [138]. More bone deposition around the implant and the formation of significantly less fibrous tissue was observed from histo-morphometry test. It was attributed to the stronger bending force, together with sol-gel surface treatment [138]. Kim et al compared the performance of DLC coated Nitinol stents with or without polyethylene glycol grafting and uncoated Nitinol stents in a canine iliac artery model. They found that implanted DLC-coated Nitinol stents induced less neointimal hyperplasia than conventional Nitinol stents [139]. Bass et al used a porcine model and studied the efficacy of a newly developed miniaturized Nitinol device as occlude inside small-diameter aorta and pulmonary arteries [140].

Most of the studies mentioned above reveal that surface treated or coated Nitinol performed better in the in-vivo biological tests however the exact reason behind this superiority was not always clearly reported. Better biocompatibility and higher corrosion resistance were the two basic and also interconnected features which offered better biological functionability of the alloy but how they actually contributed towards reducing neointimal hyperplasia in case of stenosed artery or improving better osteo-integration in case of intramedullary nails was not discussed in details. Moreover, comparative evaluation between different varieties of treated, coated or surface modified Nitinol was often quite difficult as the tests were not done under perfectly identical situations and there was contradictory results as well. More often than not, animal trials were not preceded by detailed in-vitro tests, e.g. Cell culture. As a result performance evaluation of the same type of samples in case of in-vitro and in-vivo tests could not be done. It appears that there is no dearth of literature on in-vitro tests, but comprehensive report that includes systematic studies on both is not yet available in plenty. Furthermore, number of research articles on biofunctionalization of Nitinol is comparatively less and how far it can improve in-vivo performance is not yet reported in detail.

References :

1. Buehler, W. J. Interview, 11 February 1993. Buehler.
2. Wang, F. E. Proc. First International Conference on Fracture 1965, 2, 899.
3. Tarnit D, Bîzdoac N, Îndril I, Vasilescu M. Properties and medical applications of shape memory alloys. Romanian Journal of Morphology and Embryology. 2009; 50(1):15–21.
4. Sauli K. Biocompatibility and biomechanical aspects of Nitinol shape memory metal implants. ISBN 951-42-7123-8 ISSN 0355-3221. November 2003.
5. Buehler, W. J., personal communication, 14 August 1991.
6. Hansen, M. Constitution of Binary Alloys, 2nd ed.; McGraw-Hill: New York, 1958.
7. Buehler, W. J., unpublished laboratory notebook, 5 February 1958.
8. Buehler, W. J., letter to Amy Axt Hanson, 15 June 1991.
9. Margolin, H.; Ence, E.; Nielsen, J. P. J. of Metals 1953, 191
10. Wang, F. E. Proc. First Intern. Conf. on Fracture 1965, 2, 899.
11. Barras J.D.C, Myers A. K. Nitinol – Its Use in Vascular Surgery and Other Applications. European Journal of Vascular and Endovascular Surgery. 2000; 564–569.
12. Morgan B.N. Medical shape memory alloy applications – the market and its products. Materials Science and Engineering. 2004; 16-23.
13. Haasters J, Bensmann G, Baumgart T. Current Concepts of Internal Fixation of Fractures. ed. H.K. Uthoff. Berlin, Germany :Springer-Verlag. 1980; 128–135
14. Brailovski V, Trochu F. Review of shape memory alloys medical applications in Russia. Biomedical Materials and Engineering. 1996; 291–298
15. Baumgart F, Bensmann G, Hartwig J. Mechanical Problems in Utilizing the Memory Effect for Osteosynthesis Plates. Tech. Mitt. Krupp - Forsc. Ber. 1977; 157–171
16. Pawels F. Traduction de: Gesamelte Abhandlungen zur Funktionellen Anatomie des Bewegungsapparates, ed. P.G. Maquet .Berlin, Germany :1979; 131–178.
17. Sawyer, Philip N, Page, Mark, Rudewald, Lagergren, Baselius, McCool, Halperin C, Srinivasan S. Characteristics Of The Human Heart- Design Requirements For Replacement. Transactions - American Society for Artificial Internal Organs. 1971; 470–473.
18. Haasters J, Salis-Solio G, Bensmann G. Engineering Aspects of Shape Memory Alloys. ed. T.W. Duerig et al. London, England: Butterworth-Heineman. 1990, 426–444.
19. Fukuyo S , Sairenji E, Suzuki Y, Suzuki K. Engineering Aspects of Shape Memory Alloys, ed. T.W. Duerig et al. Amsterdam: Butterworth-Heineman, 1990; 470–476.

20. Sugita Y, Shimomitsu T, Oku T, Murabayashi S, Kambic H, Harasaki H, Shirey E, Golding L, Nosé Y. Nonsurgical implantation of a vascular ring prosthesis using thermal shape memory Ti/Ni alloy (Nitinol wire). *Transactions - American Society for Artificial Internal Organs*. 1986; 30–34.
21. Oku, Takahiko, Sutton, Charles; Kambic, Helen E, Harasaki, Hiroaki, Nosé, Yukihiro. A Titanium-Nickel Alloy Intravascular Endoprosthesis In Vitro Studies. *Transactions - American Society for Artificial Internal Organs*. 1988; 399–403.
22. Palmaz J. Balloon-Expandable Intravascular Stent. *American Journal of Radiology*. 1988; 1263–1269.
23. Serruys P, ACC, Bradley H. Strauss, Heleen M, Beusekom V, Willem J, Giessen J. Stenting of Coronary Arteries: Has a Modern Pandora's Box Been Opened?. *Journal of the American College of Cardiology* . 1991; 143–154.
24. Becker G. Intravascular stents. General principles and status of lower-extremity arterial applications. *Circulation*. 1991; 122–236.
25. Tominaga R, Kambic H, Emoto H, Harasaki H, Sutton C, Hollman J. Effects of design geometry of intravascular endoprotheses on stenosis rate in normal rabbits. *American Heart Journal*. 1992; 21–27.
26. Rothman M, Davies S. Intracoronary stents. *British Heart Journal*. 1992; 425–429.
- Palmaz J. Intravascular Stents: Tissue-Stent Interactions and Design Considerations . *American Journal of Radiology*. 1993; 613–618. .
26. Lossef S., Robert J. Lutz, Mundorf J, Barth K. Comparison of Mechanical Deformation Properties of Metallic Stents with Use of Stress-Strain Analysis. *Journal of Vascular and Interventional Radiology* . 1994; 341–349.
27. Flueckige F., Sternthal H, Günter E. Klein, Szolar., Kleinhapfl G. Strength, Elasticity, and Plasticity of Expandable Metal Stents: In Vitro Studies with Three Types of Stress *Journal of Vascular and Interventional Radiology*. 1994; 745–750.
28. Hausegger K, Cragg A, Lammer J, Lafer M. Iliac artery stent placement: clinical experience with a Nitinol stent. *Radiology*. 1994; 199–202.
29. Veith F. Presidential address: Transluminally placed endovascular stented grafts and their impact on vascular surgery. *Journal of Vascular Surgery*. 1994; 855–860.
30. Marin M, Veith F, Cynamon J, Sanchez L, Bakal C, W Suggs, Lyon R, Schwartz M, Parsons R, Wengerter K, Parod J. Human transluminally placed endovascular stented grafts:

Preliminary histopathologic analysis of healing grafts in aortoiliac and femoral artery occlusive disease. *Journal of Vascular Surgery*.1995; 595–604.

31. Mak K, Belli G, Moliterno D. Subacute stent thrombosis: Evolving issues and current concepts.*Journal of the American College of Cardiology*.1996; 494–503.

32. Guidoin R, Marois Y, Douville Y, King M, Castonguay M, Traore A et al. First-Generation Aortic Endografts: Analysis of Explanted Stentor Devices From the EUROSTAR Registry. *Journal of Endovascular Therapy*.2000; 105–122.

33. Homans.*Journal of Surgery, Gynecology, Obstetrics*.1994; 70–82.

34. Simon M , Kaplow R , Salzman E, Freiman D. A Vena Cava Filter Using Thermal Shape Memory Alloy Experimental Aspects. *Radiology*.1977; 89–94.

35. Sekiguchi Y. Shape Memory Alloys, ed. H. Funakubo .Amsterdam: Gordon and Breach Science Publishers.1987; 226–269.

36. Hawkins S, Al-Kutoubi M. The simon Nitinol vena cava filter: preliminary experience in the UK. *Clinical radiology*.1992;378-380.

37. Drexel M, Selvaduray G, Pelton A.The Effects of Cold Work and Heat Treatment on the Properties of Nitinol Wire. *Medical Device Materials IV:Proceedings from the Materials & Processes for Medical Devices Conference 2007*, DOI: 10.1361/cp2007mpmd114 114.

38. Duerig T, Pelton A, Stockel D. An overview of Nitinol medical applications. *Materials Science and Engineering A*.1999; 149–160.

39. Gesenber A, Sinterman R. Management of benign prostatic hyperplasia in high-risk patients: long-term experience with the Memotherm stent. *Journal of Urology*.1998;72–76.

40. Yanagihara K, Mizuno H, Wada H, Hitimi S. Tracheal stenosis treated with self-expanding Nitinol stent. *Annals of Thoracic Surgery*. 1997; 1786–1789.

41. Yachia D. The use of urethral stents for the treatment of urethral strictures.*Annals of Urology*.1993; 27: 245–250.

42. Vinograd I, Klin B, Brosh. A new intratracheal stent made from Nitinol, an alloy with a shape memory effect. *Journal of Thoracic Cardiovascular Surgery*. 1994; 1255–1260.

43. Tack J, Gevers AM, Rutgeerts P. Self-expandable metallic stents in the palliation of rectosigmoidal carcinoma: a follow-up study.*Gastrointestinal Endoscopy*.1998; 267–271.

44. Gottfried HW, Gnann R, Brandle E. Treatment of high risk patients with subvesical obstruction from advanced prostatic carcinoma using a thermosensitive mesh stent. *British journal of Urology*.1997; 623–627.

45. Angueira CE, Kadakia SC. Esophageal stents for inoperable esophageal cancer: which to use? *American Journal of Gastroenterology*.1997; 373–376.

46. Rossi P, Bezzi M, Rossi M et al. Metallic stents in malignant biliary obstruction: results of a multicenter European study of 240 patients. *Journal of Vascular Interventional Radiology*.1994; 5: 279–285.
47. Pocek M, Mazpes F, Masala S. Palliative treatment of neoplastic strictures by self-expanding Nitinol Strecker stent. *European Radiology*.1996; 230–235.
48. Lipscomb IP, Nokes LDM. *The Application of Shape Memory Alloys in Medicine*. Norfolk. Paston Press Ltd, 1996.
49. Thompson A.S. An overview of nickel–titanium alloys used in dentistry. *International Endodontic Journal*. 2000; 297–310.
50. O’Leary J, Nicholson J, Gatturna R, Duerig T, Melton K, Stockel D, Waguian C. *Engineering Aspects of Shape Memory Alloys*. Butterworth-Heinemann, Boston.1990; 477.
51. Das G, Voss G, Jarvis G, Wyche K, Gunther R, Wilson R. Experimental atrial septal defect closure with a new, transcatheter, self-centering device. *Circulation Journal*. 1993; 1754.
52. Cuschieri A. Variable curvature shape-memory spatula for laproscopic surgery. *Surgical Endoscopy*.1991; 179–181.
53. Hagemeister N et al. First International Conference on Shape Memory and Superelastic Technologies. The International Organization on Shape Memory and Superelastic Technologies, 1994; 395–400; (Santa Clara; CA).
54. Hagemeister N et al. *Journal de Physique IV*, coll. C8, supplement *Journal de Physique III*.1995; 1223–1228.
55. Poddevin N, Marois Y, Cronier B, Delagoutte J, Guidoin R. Rupture of current ACL prostheses. A retrospective analysis of 89 surgically excised explants. *Polymers & Polymer Composite*.1995; 79–97.
56. Hagemeister N, Yahia L, Lours T. *Journal de Physique IV*. coll.C2, Supplement *Journal de Physique III*.1995; 403–408.
57. Trépanier C, Tabrizian M, Yahia L, Bilodeau L, Piron D. Improvement of the Corrosion Resistance of NiTi Stents by Surface Treatments. *Materials Research society Symposium Proceedings*.1997; 363.
58. Trigwell A, Selvaduray G, Pelton A, Hodgson D, Russel R, Duerig T. *Proceedings of the 2nd International Conference on Shape Memory and Superplastic Technologies, SMST-1997*; 387; Pacific Grove, CA.
59. Chan C, Trigwell S, Duerig T. Oxidation of an NiTi alloy. *Surface and Interface Analysis*. 1990;349.

60. Lausmaa J, Mattsson L, Rolander U, Kasemo B. Chemical Composition And Morphology Of Titanium Surface Oxides. *Materials Research Society Symposium Proceedings*.1986; 351.
61. Espinos J, Fernández A, González A. Elipse Oxidation and diffusion processes in nickel-titanium oxide systems. *Surface Science*.1993; 420.
62. Barrett R, Bishara S. Biodegradation of orthodontic appliances. Part I. Biodegradation of nickel and chromium in vitro, *American Journal of Orthodontics and Dentofacial Orthopedics*.1993; 8.
63. Bishara S, Barrett R, Selim M. Biodegradation of orthodontic appliances. Part II. Changes in the blood level of nickel, *American Journal of Orthodontics and Dentofacial Orthopedics*. 1993; 115.
64. Trepanier C, Leung T, Tabrizian M, Yahia L, Bienvenu J, Tanguay J, DPiron L, Bilodeau L. Preliminary investigation of the effects of surface treatments on biological response to shape memory NiTi stents. *Journal of Biomedical Materials Research*.1999;165.
65. Fukuyo S, Duerig T, Melton K, Stockel D, Waguian C. *Engineering Aspects of Shape Memory Alloys*. Butterworth-Heinemann, Boston.1990; 470.
66. Weve D, Veldhuizen A, Vries J, Busscher H, Uges D, van Horn J. Electrochemical and surface characterization of a nickel–titanium alloy. *Biomaterials*.1998;761.
67. H. Sakamoto et al. US Patent. 4 925 445.1990.
68. Stockel D. *Minimally Invasive Therapy & Allied Technology*.2000; 81-88.
69. Chute J, Duerig T, Melton K, Stockel D, Waguian C. *Engineering Aspects of Shape Memory Alloys*. Butterworth-Heinemann, Boston, 1990; 420.
70. Burstone C, ed. Graber T, Swain T. *Current Concepts and Techniques*. vol. 2, (St. Louis, MO: Mosby). 1985; 23–38.
71. Eugene S F., Huget Laszlo B. Desimon. Potential Applications Of Certain Nickel-Titanium (Nitinol) Alloys. *Journal Of Dental Research*.1975; 89–96.
72. Andreasen G, Barrett R. An evaluation of cobalt-substituted Nitinol wire in orthodontics. *American Journal of Orthodontics* .1973; 462–47.
73. Sachdeva R, Miyazaki S. *Engineering Aspects of Shape Memory Alloys*.ed. T.W. et al. (Stoneham, MA: Butterworth-Heineman,). 1990; 452–469.
74. Shabaloskya S. *Applications Medicales des Materiaux Intelligents*, Montreal, Canada, 8 December 1995.
75. Simske S, et al., in. Pelton A, Hodgson D, Duerig T (Eds.). *Proceedings of the 1st International Conference on Shape Memory and Superplastic Technologies, SMST-94, SMST proceedings*, Pacific Grove, CA, 1994;. 449

76. Mahtabi M, Shamsaei N, Mitchell M. Fatigue of Nitinol: the state-of-the-art and ongoing challenges. *Journal of the Mechanical Behavior of Biomedical Materials*.2015; 228–254.
77. Pelton A, Schroeder V, Mitchell M, Gong X, Barney M, Robertson S. Fatigue and durability of Nitinol stents.*Journal of the Mechanical Behavior of Biomedical Materials*.2008 ;153–164.
78. Li S, Cui T, Hao Y, Yang R. Fatigue properties of a metastable β -type titanium alloy with reversible phase transformation, *Acta Biomaterialia*. 2008; 305–317.
79. Wadood A. Brief Overview on Nitinol as Biomaterial. *Advances in Materials Science and Engineering*. 2015; 9 pages.
80. Laste Zr, MacBean A, Ayliffe P, L. C. Newlands, Fixation of a frontozygomatic fracture with a shape-memory staple. *British Journal of Oral and Maxillofacial Surgery*.2001; 324–325
81. Wiebking, Stapel N, Hurschler C, Gösling T. Rotation resistance of new intramedullary nail made from shape memory alloy depends upon the bone diameter. O. Dössel, W C. Schlegel (Eds.): *WC 2009, IFMBE Proceedings* .2009.
82. Dai KR, Hou XK, Sun YH et al. Treatment of intra-articular fractures with shape memory compressive staples. *Injury* 1993; 651-655
83. P. Xue, F. Yunyue, Y. Danhua. *Shape Memory Alloy*. 1986 ; 444–446.
84. Schmerling M, Wilkov M, Sanders A, Woosley J. Using the shape recovery of Nitinol in the Harrington rod treatment of scoliosis. *Journal of Biomedical Materials Research*.1976;.879–892.
85. Schmerling MA, Wilkor MA, Sanders AE, Woosley JE. Medical application of the shape memory effect: An Ni-Ti Harrington rod for treatment of scoliosis. *Journal Of Biomedical Materials Research*.1976; 879–902.
86. Sanders JO, Sanders AE, More R et al. A preliminary investigation of shape memory alloys in the surgical correction of scoliosis. *Spine*. 1993; 1640–1646.
87. Chiu KY, Wong MH, Cheng FT, Man HC. Characterization and corrosion studies of titania-coated NiTi prepared by sol-gel technique and steam crystallization. *Applied Surface Science*.2007; 6762–8.
88. Trepanier C, Tabrizian M, Yahia LH, Bilodeau L, Piron DL. Effect of modification of oxide layer on NiTi stent corrosion resistance. *Journal Of Biomedical Materials Research*. 1998;433–40.
89. Armitage DA, Grant DM. Characterisation of surface-modified nickel titanium alloys. *Material Science And Engineering A*.2003;89–97.

90. Thierry B, Tabrizian M, Savadogo O, Yahia L. Effects of sterilization processes on NiTi alloy: surface characterization. *Journal Of Biomedical Materials Research*.2000; 88–98.
91. Thierry B, Tabrizian M, Trepanier C, Savadogo O, Yahia L. Effect of surface treatment and sterilization processes on the corrosion behavior of NiTi shape memory alloy. *Journal Of Biomedical Materials Research*.2000;685–93.
92. Bansiddhi A, Sargeant T, Stupp S, Dunand D. Porous NiTi for bone implants: A review ,*Acta Biomaterialia*. 2008 ; 773–782
93. Cempel M, Nickel G. Nickel: a review of its sources and environmental toxicology. *Polish Journal Of Environmental Studies*. 2006;375–82.
94. Denkhaus E, Salnikow K. Nickel essentiality, toxicity, and carcinogenicity. *Critical Reviews in Oncology/ Hematology*. 2002;35–56.
95. Meng Q, Liu Y, Yang H, Shariat B, Nam T. Functionally graded NiTi strips prepared by laser surface anneal. *ActaMaterialia*. 2012; 1658–1668.
96. Yan X, Yang Z. Corrosion resistance of laser spot-welded joint of NiTiwire in simulated human body fluids. *Journalof Biomedical Materials Research*.2006; 97–102.
97. Man H, Cui Z, Yue T. Corrosion properties of laser surface melted NiTi shape memory alloy.*ScriptaMaterialia*. 2001; 1447–1453.
98. Sevilla P, Martorell F, Libenson C, PlanellJ,Gil F. Laser welding of NiTi orthodontic archwires for selective force application. *Journal of Material Science: Materials in Medicine*. 2008; 525–529.
99. Cui Z, Man H, Yang X. The corrosion and nickel release behavior of laser surface melted NiTi shape memory alloy in Hanks, solution. *Surface Coating Technology*.2005; 347–353.
100. Budziak D, Martendal E, Carasek E. Preparation and application of NiTi alloy coated with ZrO₂ as a new fiber for solid-phase microextraction. *Journal of Chromatography A*. 2007; 18–24.
101. Shabalovskaya S. Physicochemical and biological aspects of Nitinol as a biomaterial. *International Materials Review*. 2001; 1 - 18.
102. Katic J, Metikos M, Hukovic, RankoBabic. Synthesis and characterization of calcium phosphate coatings on Nitinol.*Journal of Applied Electrochemistry*.2014 ;87–96.
103. Jiang H, Rong L. Effect of hydroxyapatite coating on nickel release of the porous NiTi shape memory alloy fabricated by SHS method. *Surface & Coatings Technology*.2006; 1017–1021.

104. Roy R, Faruque S, Ahmed, Woo Yi J, Moon M, Lee K, Jun Y. Improvement of adhesion of DLC coating on Nitinol substrate by hybrid ion beam deposition technique. *Vacuum*.2009; 1179–1183.
105. Sui J, Cai W, Zhao L. Surface modification of NiTi alloys using diamond-like carbon (DLC) fabricated by plasma immersion ion implantation and deposition (PIIID).*Nuclear Instruments and Methods in Physics Research*.2006; 67–70.
106. Liu C, Hu D, Xu J, YangD,Qi M. In vitro electrochemical corrosion behavior of functionally graded diamond-like carbon coatings on biomedical Nitinol alloy.*Thin Solid Films*.2006; 457 – 462.
107. Bakhshi R, Darbyshire A, Evans J, You Z,Lu J, Alexander M. Seifalian, Polymeric coating of surface modified Nitinol stent with POSS-nanocomposite polymer. *Colloids and Surfaces B: Biointerfaces* .2011; 93–105.
108. Gill P, Musaramthota V, Munroe N, Datye A, DuaR,Haider W, McGoron A, Rokicki R. Surface modification of Ni–Ti alloys for stent application after magnetoelectropolishing. *Materials Science and Engineering C*. 2015; 37–44.
109. Shen Y, Wang G, Chen L, Li H, Yu P, Bai M, Zhang Q, Lee J, Yu Q. Investigation of surface endothelialization on biomedical Nitinol (NiTi) alloy: Effects of surface micropatterning combined with plasma nanocoatings. *ActaBiomaterialia*.2009; 3593–3604.
110. Schmehl J, Harder C, Wendel H, Claussen C, TepeVG. Silicon carbide coating of Nitinol to increase antithrombogenicproperties and reduce nickel release. *Cardiovascular Revascularization Medicine*.2008; 255-262.
111. Villiermaux F, Tabrizian M, Yahia L, Meunier M, PironD.Excimer laser treatment of NiTi shape memory alloy biomaterials. *Applied Surface Science*.1997; 62–66.
112. Pequegna A, Michael A, Wang J, Lian K, Zhou Y, Khan M. Surface characterizations of laser modified biomedical grade NiTi shape memory alloys. *Materials Science and Engineering C*.2015; 367–378.
113. Petrović S, Peruško D, Kovač J, Panjan M, Gaković B, Radak B, Janković-Mandić L, Trtica M. Laser treatment of nanocomposite Ni/Ti multilayer thin films in air. *Surface & Coatings Technology* .2012; 93–97.
114. Tulloch A, Chun Y,Levi D, Mohan chandra K, Carman G, Lawrence P, Rigberg D. Super Hydrophilic Thin Film Nitinol demonstrates Reduced Platelet Adhesion Compared with Commercially Available Endograft Materials. *Journal of Surgical Research*.2011; 317–322.

115. Chrzanowski W, Neel E, Armitage D, Lee K, Walke W, Knowles J. Nanomechanical evaluation of nickel–titanium surface properties after alkali and electrochemical treatments. *Journal of the Royal Society Interface*. 2008 ; 1009–1022.
116. M.Li, Y.B, Wang, Zhang X, Li Q, Liu Q, Y Cheng, Zheng Y, Xi T, Wei S. Surface characteristics and electrochemical corrosion behaviour of NiTi alloy coated with IrO₂. *Material science and engineering C*. 2013; 15-20.
117. Shabalovskaya S, Rondelli G, Undisz A, Anderegg J, Bulreigh T, Rettenmayr M. The electrochemical characteristics of native Nitinol surfaces. *Biomaterials*. 2009; 3662-3671.
118. Zein S, Abeidin E, Welz-Biermann U, Endres F. A study on the electrodeposition of tantalum on Nitinol alloy in an ionic liquid and corrosion behaviour of the coated alloy. *Electrochemistry communications*. 2005; 941-946.
119. Zhao C, Pandit, Fu Y, Mijakovic I, Jesorka A, Liu J. Graphene oxide based coating on Nitinol for biomedical implant applications :effectively promote mammalian cell growth but kill bacteria. *Royal society of chemistry Advances* .2016; 38124.
120. Kong X, Grabitz R, Oeveren W, Klee D, Van T, Kooten, Freudenthal F, Qing M, Bernuth G, Seghaye M. Effect of biologically active coating on biocompatibility of Nitinol devices designed for the closure of intra-atrial communications. *Biomaterials*. 2002; 1775–1783.
121. Karaji, Speirs M, Dadbakhsh S, Kruth J, Weinans H, Zadpoor A, Yavari S. Additively Manufactured and Surface Biofunctionalized Porous, Nitinol. *Applied materials and interfaces*. 2017; 1293-1304.
122. Devillers S, Barthélémy B, Fery I, Delhalle J, Mekhalif Z. Functionalization of Nitinol surface toward a versatile platform for post-grafting, chemical reactions. *Electrochimical Acta*. 2011; 8129–8137.
123. Chua P, Neoh K, Kang E, Wang W. Surface functionalization of titanium with hyaluronic acid/chitosan polyelectrolyte multilayers and RGD for promoting osteoblast functions and inhibiting bacterial adhesion. *Biomaterials*. 2008; 1412-1421.
124. Lutz R, Srour S, Nonhoff J, Weisel T, Damien CJ, Schlegel KA. Biofunctionalization of titanium implants with a biomimetic active peptide (P-15) promotes early osseointegration. *Clinical Oral Implants Research*. 2010; 726–734.
125. Yazici Q, Fong B.H, Wilson, Oren E, Amos F, Zhang H, Evans J, Snead M, Sarikaya M, Tamerler C. Biological response on a titanium implant-grade surface functionalized with modular peptides. *Acta Biomaterialia* .2013; 5341–5352.

126. Auernheimer J, Zukowski D, Dahmen C, Kantlehner M, Enderle A., Simon L. Goodman, and Kessler H, Titanium Implant Materials with Improved Biocompatibility through Coating with Phosphonate-Anchored Cyclic RGD Peptides, *ChemBioChem* 2005, 6, 2034 – 2040.
127. Germanier Y, Tosatti S, Broggin N, Textor M, Buser D. Enhanced bone apposition around biofunctionalized sandblasted and acid-etched titanium implant surfaces. A histomorphometric study in miniature pigs, *Clin.OralImpl. Res.* 17, 2006; 251–257.
128. Herranz-Diez C, Li, C Q. Lamprecht, Mas-Morunoc C, Eubauer S, Kessler H, Manero J, Guillem-Martí J, Selhuber-Unkel C. Bioactive compounds immobilized on Ti and TiNbHf: AFM-based investigations of biofunctionalization efficiency and cell adhesion. *Colloids and Surfaces B: Biointerfaces.* 2015; 704–711.
129. Nathalia Marín-Pareja, Emiliano Salvagni, Jordi Guillem-Martí, Conrado Aparici, Maria-Pau Ginebra., Collagen-functionalised titanium surfaces for biological sealing of dental implants: Effect of immobilization process on fibroblasts response, *Colloids and Surfaces B: Biointerfaces* 122 (2014) 601–610.
130. Bagnò A, Piovan A, Dettin M, Chiarion A, Brun P, Gambaretto R, Fontana G, Bello C, Palù G, Castagliuolo I. Human osteoblast-like cell adhesion on titanium substrates covalently functionalized with synthetic peptides. *Bone.* 2007; 693–699.
131. Arroyo-Hernández M, Martín-Palmaa R, Pérez-Rigueiro J, García-Ruiz J, García-Fierro J, Martínez-Duárden J. Biofunctionalization of surfaces of nanostructured porous silicon. *Materials Science and Engineering Materials Science and Engineering C.* 2003; 697–701.
132. Zhang F, Kang ET, Neoh KG, Wang P, Tan KL. Surface modification of stainless steel by grafting of poly(ethylene glycol) for reduction in protein adsorption. *Biomaterials.* 2001; 1541–1548.
133. Zhao C, Pandit S, Fu Y, Mijakovic I, Jesorka A, Liu J. Graphene oxide based coating on Nitinol for biomedical implant applications: effectively promote mammalian cell growth but kill bacteria. *Royal society of chemistry Advances.* 2016; 38124.
134. Simsek Yilmaz S, Liehn E, Weinandy S, Schreiber F, Megens R, Theelen W, Smeets W, Jockenhövel S, Gries T, Möller M, Klee D, Weber C, Zerneck A. Targeting In-Stent-Stenosis with RGD- and CXCL1-Coated Mini-Stents in Mice, *PLOS:ONE.* 2016.
135. Takeshita F, Takata H, Ayukawa Y, Suetsugu. Histomorphometric analysis of the response of rat tibiae to shape memory alloy (Nitinol). *Biomaterials.* 1997; 21-25.

136. Trepanier C , Leung T, Tabrizian, Yahia L, Bienvenu J, Tanguay J, PironD,BilodeauL. In vivo biocompatibility study of niti stents. Proceedings of the 2nd Int’l Conference on Shape Memory and Superelastic Technologies (eds.).1997;423-428.
137. Thierry B, Merhi Y, Bilodeau L, Trepanier C, Tabrizian M. Nitinol versus stainless steel stents: acute thrombogenicity study in an ex vivo porcine model. *Biomaterials* 2002; 2997–3005.
138. Muhonen V, Kujala S, Vuotikka A , Aritalo V, PeltolaT, Areva S, Narhi T, Tuukkanen J. Biocompatibility of sol–gel-derived titania–silica coated intramedullary NiTi nails. *Acta Biomaterialia*.2009; 785–793.
139. Kim J, Shin J, Shin, Moon M, Park K, Kim, Shin K, Won Y, Han D, Lee K. Comparison of diamond-like carbon-coated Nitinol stents with or without polyethylene glycol grafting and uncoated Nitinol stents in a canine iliac artery model. *The British Journal of Radiology*.2011; 210–215.
140. Bass J, Wilson N. Transcatheter Occlusion of the Patent Ductus Arteriosus in Infants: Experimental Testing of a New Amplatzer Device. *Catheterization and Cardiovascular Interventions*. 2014 ; 250–255 .

**CHAPTER 3:
SCOPE OF THE WORK &
OBJECTIVE**

Scope of the work

From previous literatures, it has been found that Nitinol is commercially an important alloy for medical implant purpose and its surface should be modified in such a way that its corrosion resistance property increases as well as its mechanical and biological properties get better for long term applicability. It is clear from literature that Ni⁺ leaching is harmful for our body. Various techniques are present to modify the nitinol surface. Literature does not reveal the comparative evaluation between different varieties of treated, coated or surface modified Nitinol. Comparative evaluation is often quite difficult as the tests were not done in perfectly identical situations and there are contradictory results as well. And sometimes animal trials were not preceded by detailed in-vitro tests. Due to this the performance valuation of the same type of samples in case of in-vitro and in-vivo tests could not be done. Extensive literature study reveals that there is no dearth of literature on in-vitro tests, but comprehensive report that includes systematic studies on both is not yet available in plenty. Moreover none has reported the performance of silanization alone. No report on the comparative performance analysis of bare and silanized is available till date.

The present study proposes to evaluate the in-vitro and in-vivo performance of bare, silanized and HAp coated Nitinol samples in a details and systematic way.

The objectives of the present study are:

- To modify the surface of Nitinol by different techniques.
- To evaluate and compare the in-vitro performance of bare nitinol, silanized nitinol and HAp coated nitinol.
- To evaluate and compare the in-vivo performance of bare nitinol, silanized nitinol and HAp coated nitinol in rabbit model over a period of three months.

Depending on the above mentioned objectives it is expected that the present study would be able to generate a robust and systematic database on physical, mechanical and biological properties of three varieties of nitinol samples. This database will provide a platform to search the prospect of real life use of nitinol in orthopaedic area. The selection of cell line and also the pattern of animal trial indicate towards the possibility of developing nitinol based orthopaedic implants in future. It is a well known fact that nitinol is a shape memory alloy and offers good mechanical properties like kink resistance, high endurance limit. These properties when coupled with the finding of the present study may provide a practical scope to use nitinol as intramedullary nails/pins in future.

CHAPTER 4:
MATERIALS & METHODS

Materials and Methods:

Methodology part of this entire study is separated into different areas as mentioned below:

- (a) Nitinol : Characterisation and surface preparation
- (b) Silanization of nitinol and its characterization
- (c) Optimization of electrophoretic deposition technique for developing Hydroxyapatite-coating on Nitinol surface and its characterization.
- (d) Comparative study on the surface properties and in-vitro, in-vivo biological performance of bare nitinol, silanized Nitinol and Hydroxyapatite coated Nitinol.

3.1. Materials: The material for these experiments was commercially available nitinol shape memory wire with 1.5 mm diameter. That nitinol alloy wire was reported to consist of 54.5 wt% Ni and 45.5 wt% Ti (Manufacturer: Nitinol Devices & Components, NDC, California; Supplier: VRAS traders, India). As per the specification of the supplier, the composition conforms well to ASTM F-2063. Another variety of same grade of Nitinol in the form of sheet with 6cm length 2 cm. width was also procured (Manufacturer: Memry Corporation, USA).

3.2 Methods:

3.2.1. XRD: X-ray crystallography of Nitinol pieces was conducted using Rigaku diffractometer, Model-UltimaIII, Rigaku Co., Tokyo, Japan.

3.2.2. Surface preparation: The NiTi wire of 1.5 mm diameter was cut into number of pieces with length 1 cm each followed by washing thoroughly for 15 min with acetone (70% by volume), ethanol, and deionized water, respectively. These washing processes were done to get rid of residual surface impurities and then finally dried to use for coating and other various studies. Before sterilization/washing processes the samples which were used for coating were polished with SiC paper. Same steps were followed in case of Nitinol sheet.

3.2.3. EDXA : EDXA study of bare Nitinol, silanized Nitinol and coated Nitinol was done using Carl Zeiss Supra35VP.

3.2.4. Silanization process: Nitinol samples were silanized by immersing into 2% v/v solution of APTES ((3-aminopropyl)triethoxy saline) (Sigma-Aldrich, St. Louis, Missouri), in toluene(Merck) for 10 hrs to produce an amino-silane surface. After that, the silanized nitinol surface was washed three times with pure toluene to remove the excess APTES. To

remove toluene from the silanized nitinol samples, the samples were washed two times with ethanol(Merck) and finally the samples were rinsed two times using deionized water (Nice chemicals(p)ltd.) to remove ethanol.

To confirm the presence of Si, the X-ray photoelectron spectroscopy (XPS) study (PHI5000 Versa Probe II, Ulvac-Phi Inc., Chigasaki, Japan) was done on silanized samples. AlK α -monochromatized x-ray source ($h\nu=1486.6$ eV) was used on the PHI5700 Physical Electronics spectrometer. The energy resolution of the spectrometer was about 0.35 eV. Samples were cleaned before the study using Ar⁺ ion beam sputtering with energy 1.5 keV and 0.7 eV by 10 and 1 minutes, respectively. The survey spectra were recorded in the wide range of binding energy 0-1400 eV. The high resolution spectra of the core lines of Fe2p, Cr2p, N1s, Si2p, P2p, O1s and C1s were measured at pass energy of 23.50 eV. The atomic concentrations were calculated by MUTLIPAK software (ver. 9.7.0.1).

3.2.5. Synthesis of Hydroxyapatite : Hydroxyapatite powder was prepared through standard wet chemical method. In this method, A.R. grade Calcium Hydroxide (Ca(OH)₂) (EMERCK, India) and ortho-phosphoric acid (H₃PO₄) (EMERCK, India) were used as starting materials. To synthesis HAp, required amount of Ca(OH)₂ was mixed gently in boiled distilled water. After proper mixing, 0.6M H₃PO₄ was added drop by drop into calcium hydroxide aqueous solution in stirring condition. The reaction was carried out at 80°C and pH was maintained at 11-12. After finishing the process, the solution was left for 24 hours for aging. After that gel like white precipitation was observed and it was filtered. During filtering the filtrate was washed repeatedly to remove any unreacted chemicals. Then the filtered cake was taken in petri dish and dried in hot air oven for another 24 hours. HAp powder was prepared by crushing the dried cakes and sieving. The as prepared HAp powder was calcined at 800°C with dwelling time 2 hours in electric furnace (NASKAR & Co., Model No.-EN170QT) to obtain the optimum crystallinity. Figure 1 shows the steps of HAp powder preparation.

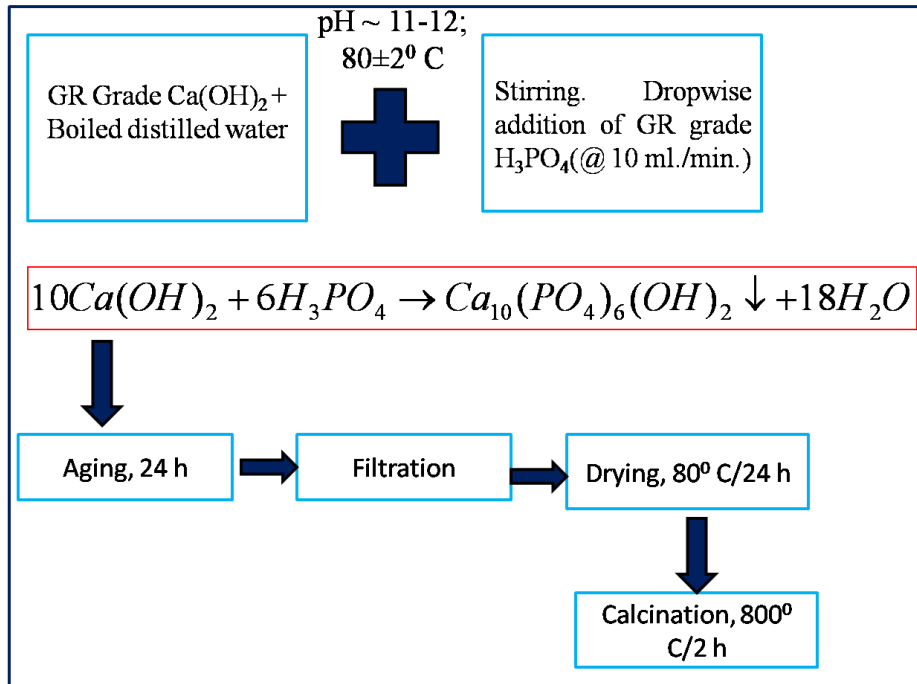


Figure 3.1: Flow chart of HAp powder preparation

3.2.6.Characterization of HAp powder:

3.2.6.1. X-Ray diffraction analysis: Pure hydroxyapatite was characterized after calcination. The composition of powder was studied using X-Ray diffraction (XRD; Rigakudiffractometer, Model-UltimaIII, Rigaku Co., Tokyo, Japan) using Cu K α 1 monochromatic X rays ($\lambda=0.154059$ nm) generated at 55 mA and 40 kV. Scans were recorded from diffraction angle (2θ) of 10° -80°, at a speed of 40/min with step size of 0.050.

The lattice parameters (a and c) of the sample were calculated from peaks (3,0,0) and (0,0,2) respectively applying the equation for hexagonal system using the method of least squares [1].

$$\frac{1}{d^2} = \frac{4}{3} \left(\frac{h^2 + hk + k^2}{a^2} \right) + \frac{l^2}{c^2} \text{----- (1)}$$

The volume (V) of the hexagonal unit cell of each HAp formulation was calculated using standard crystallographic equation $V=2.589a^2c$ [1].

Degree of crystallinity of powders was calculated by using the following relationships [2]:

$$X_c = 1 - \frac{V_{112/300}}{I_{300}} \text{----- (2)}$$

Where: I_{300} is the intensity of (300) plane reflection and $V_{112/300}$ is the intensity of the hollow between the planes (112) and (300) reflections. Crystallite size was calculated by using full width at half maxima (FWHM) method. [1]. Taking into account, the broadening of each peak for both a and c axis peaks in XRD mean crystalline size has been calculated.

3.2.6.2. Fourier Transform Infrared Spectroscopy (FTIR) analysis: The functional groups of HAp were analyzed by Fourier Transform Infrared Spectroscopy (FTIR) which was obtained by using Perkin-Elmer, Model 1615 (USA) instrument. HAp powder was dispersed with pre-dried KBr in the proportion of 10 wt.% for measurements. Background noise was corrected with pure KBr data. The measuring resolution was 4 cm^{-1} and 256 readings were performed in the range from 400 to 4000 cm^{-1} .

The particle size distribution was measured using Malvern instrument (ZEN 3690).

3.2.7. Electrophoretic deposition process: To prevent the gas formation due to the hydrolysis of water, 99% ethanol was used as a solvent during electrophoresis resulting in the deposition of uniform adherent hydroxyapatite coatings [3,4]. The colloidal suspension was placed in a magnetic stirrer for 60 min and after that in an ultrasonic bath for 60min. Hydroxyapatite from the colloidal suspension was deposited on NiTi samples using the electrophoresis (EPD) technique. The NiTi substrate was used as a cathode and as a counter electrode also. The electrodes were placed parallel to each other within a distance of 15 mm and connected to the power supply enabling current measurements. The standardized voltage for this work was 60volts and deposition time was 90minutes with number intermittent drying after every 10 minutes. All EPD experiments were carried out at room temperature. After deposition, the green coatings were dried with normal dryer for few minutes and after getting the desired coating the samples were finally dried at 80°C for 2 hrs.



Figure 3.2 : Electrophoretic deposition technique

Using Rigaku diffractometer, Ultima-III, Rigaku Co., Tokyo, Japan X-ray diffraction analysis was done on the deposited powder to check if there was any change in the form of hydroxyapatite after electrophoresis.

3.2.8. 3-D Profilometry Study: Surface textures of bare nitinol, silanized Nitinol and **coated** Nitinol were studied using non-contact non destructive three-dimensional laser profilometer (Bruker Contour GT with Vision 64 software) prior to further detailed in-vitro and in-vivo studies.

3.2.9. Leaching study: In a freshly prepared phosphate buffer solution (PBS) [5] leaching studies of Bare Nitinol, Silanized Nitinol and coated Nitinol were done for a period of seven days by using Atomic absorption spectroscopy (Perkinelmer, Model No. pinaacle 900F). Data were taken on intermittently on 1st day, 7th day.

3.2.10. Contact angle measurement: In the static mode, at room temperature(25 °C) sessile drop technique (DSA4, Kruss Easy drop) was used to measure the contact angle of bare Nitinol, silanized Nitinol and coated Nitinol surface. Probe liquid was distilled water. For each surface, the contact angle was measured at number of spots. All the data are expressed as mean \pm S.D.

3.2.11. In-vitro Cell culture study: Human osteoblast-like cells (MG 63) were procured from National Centre for Cell Science (NCCS), Pune, India and following the standard protocol, the cells were preserved.

In- vitro cell culture study was performed in two parts. In 1st part, the in-vitro cell culture study was done with bare and silanized nitinol for two days and it was repeated with all three samples, bare, silanized and HAp coated nitinol for a span of 5days where data were taken on intermittently on 1st and 5th day.

3.2.11.1. 1st Part: In this study the MG63 osteoblast cell line was used. The viability of the MG-63 cells (human osteoblast cell) on the NiTi samples were tested for 48 hours. Nitinol samples were cast into the wells of a 24-well plate (Tarsons, India). MG-63 cells were maintained in incomplete Dulbecco's modified eagle media ((DMEM), Gibco by life technologies), (10% Fetal Bovine Serum (FBS, Himedia) and 1% antibiotic solution (penicillin, streptomycin, antimycin)) at 37°C, 5% CO₂, 95% humidity. Cells were harvested by trypsinization (Himedia) and 1X10⁴ cells were seeded to each well of a 24-well plate and incubated for 12hrs for adherence (37°C, 5% CO₂ and 95% humidity). NiTi samples

at a concentration of 100µg/ml were added to the adhered cells in respective wells for a period of 48hours. The complete media was taken as control.

3.2.11.2. MTT assay: Using MTT assay kit (Himedia, Mumbai, India) following manufacturer's instruction, MTT assay was carried out at definite time interval. Dissolving the formed formazan crystals in DMSO (100µl) the absorbance was measured at 595nm. Cell proliferation was expressed in terms of the cell proliferation index (CPI). The data was reported in terms of CPI.

$$\text{CPI} = \text{OD}_{\text{test}} / \text{OD}_{\text{control}}$$

3.2.11.3. Cell Count: For cell count, the cells were trypsinised first and then we added complete media to the cells. Then it was centrifuged for 3minutes and then the supernatant was discarded. After that complete media was added and 10µl cell suspension was taken from that. It was put into hemocytometer and counting of cells under the phase microscope (Axiocam ERc5s, Zeiss) was done.

3.2.11.4. Immunocytochemistry: In a 24well plate MG-63 cells (1X10⁴cells/well) were seeded. The seeded cells were kept in the incubator for a period of 12 hrs for adherence. Thereafter, in the adhered cells Nitinol samples were added. After 24hrs, cells were first fixed with 4% paraformaldehyde, permeabilized, and then subjected to 15minutes incubation with gentle shaking. After fixing, the samples were washed with PBS thrice. Then 0.25% Triton X was added and subjected to 15minutes incubation with gentle shaking. Finally, the samples were washed thrice with PBS and counter-stained with DAPI (4', 6-diamidino-2-phenylindole, 0.2-2µg/ml, 50µg/ml) and TRITC (tetramethylrhodamineisothiocyanate) Phalloidin. The expressions were visualized using a fluorescence microscope (IX 71,Olympus). Analysis of the expressions from fluorescence micrographs was done using standard Image-J software.

3.2.11.15. 2ndpart : Before cell seeding the scaffolds were sterilized by 70% ethanol and UV light treatment for 30 min. Scaffolds were then conditioned with DMEM for 2 hr to home the cells better. This was followed by several washings with sterile PBS (pH 7.4). DMEM (Dulbecco's Modified Eagle's Medium), containing 10% fetal calf serum and 1% penicillin/streptomycin, was used to maintain MG63 cell line at 37°C in 5% CO₂ humidified atmosphere. After getting confluence, MG63 cells were trypsinized and counted with a Automated cell counter (TC10, Bio-RAD Laboratories). Each sample was transferred into

the respective well of a 48 well plate and seeded onto their surface in a drop wise manner at a cell density of 1.7×10^6 cells/scaffold. To promote cell adhesion the cell seeded scaffolds were kept in humidified atmosphere at 37°C in 5% CO₂ for 1h. Finally, the constructs were maintained in DMEM . The culture media were renewed on every alternate day.

3.2.11.16. MTT analysis: A quantitative colorimetric measurement of extracellular reduction of the yellow colored Tetrazolium dye 3-[4, 5-dimethylthiazol-2-yl]-2, 5-diphenyl tetrazoliumbromide (MTT, Himedia India) to insoluble purple formazan crystals was performed to analyze cell viability percentage. MTT-assay was prepared in phosphate buffer solution (PBS) at a concentration of 4.2 mg/ml and 100 µl of this solution was mixed with 400 µl of cell culture media and poured in each well of the 48 well-plate with the cells. Further, well-plate was incubated inside 5% CO₂ incubator at 37°C for 4 hours. Afterwards, media was discarded and residual water-insoluble formazan crystals were dissolved in 200 µl of dimethylsiloxane (DMSO) in each well. After vigorously mixing the crystals in DMSO a purple solution is formed which was transferred into a 96 well plate for colorimetric reading in spectrophotometer plate-reader (Multiskan GO, Thermo Fisher Scientific, India).

3.2.11.17. Confocal Study: Cell proliferation study of osteoblast cells was conducted using confocal microscope. The confocal laser pictographs were obtained after 5 days of culture period. All the samples were fixed with 4% paraformaldehyde at room temperature for 20 minutes and washed with 1X PBS three times. Next, samples were permeabilized with 0.1 % Triton X-100 for 10 minutes and again washed with PBS thrice. Blocking agent 1% BSA was added to each samples to reduce background noise for 1 h followed by Rhodamine Phalloidin (Invitrogen™, Thermo fisher Scientific) staining with time duration of 45 minutes which were washed properly with PBS. For nucleus staining DAPI was used for 5-10 minutes and again washed with PBS. All the samples were stored in PBS at 4 °C until imaging.

3.2.12. In-vivo animal trial: Animal trial was carried out following the techniques conforming to the standards of the Institutions' Animal Ethical Committee of the West Bengal University of Animal and Fishery Sciences, Kolkata, India(Permit No. Pharma/188 (ix) dated 31.07.2015). Bone samples were harvested after one month (1M) and three month (3M).

Table 3.1: Sample type

Sample 1	Bare Nitinol
Sample 2	Silanized Nitinol
Sample 3	Electrophoretically deposited HAp coated Nitinol

3.2.12.1. Preparation of samples: The NiTi wire of 1.5 mm diameter was cut into number of pieces with length 1 cm each followed by washing thoroughly for 15 min with acetone (70% by volume), ethanol, and deionized water, respectively, to remove residual surface impurities and finally dried to use as implant.

3.2.12.2. Surgery and implantation procedure: Twenty healthy New Zealand white rabbits of both genders, weighing 2–2.5 kg were randomly divided into four groups:

Table 3.2: Animal group type:

Group I	Control group
Group II	Test animals with Bare Nitinol implant
Group III	Test animals with Silanized Nitinol implant
Group IV	Test animals with electrophoretically HAp coated Nitinol implant

The specimen was implanted transversely within the created defects in the distal epiphysis of femur. Prior to surgery, the rabbits kept individually in separate cages with alternating 12 h cycles of light and dark in temperature and humidity-controlled rooms, given water ad libitum and were without restriction of movement. Anaesthesia was achieved by injecting a dose of 1 mg/kg body weight of xylazine hydrochloride (XYLAXIN®, Indian Immunologists Ltd., Ahmedabad, India) and ketamine hydrochloride (Ketalar®, Parke-Davis, Hyderabad, India) at a dose of 25 mg/kg body weight intramuscularly. A bone defect (5X1.5 mm) in each animal was created in the medial aspect of the distal epiphysis of femur bone with the help of a motorized dental drill. The implant was inserted in a press fit manner within the created bone defects and secured in position by suturing muscle, subcutaneous tissue, and skin in layers.

3.2.12.3. Local inflammatory reaction and healing of wound: All the animals were closely observed for lameness and weight bearing capacity, swelling of the surgical area and related signs of local inflammatory reactions were observed from the day of operation postoperatively, and changes were evaluated by visual and manual examinations. All the treated animals were administered using injection, cefotaxime sodium (Mapra India, Kolkata, India) at a dose rate 65 mg per animal intramuscularly, at 12 h interval daily for 5 days and meloxicam (MELONEX®, Intas Pharmaceuticals, Ahmedabad, India) at 0.2 mL once daily for 5 days. Dressing of surgical wounds was carried out using povidone iodine lotion and antibiotic ointment for 10 days postoperatively.

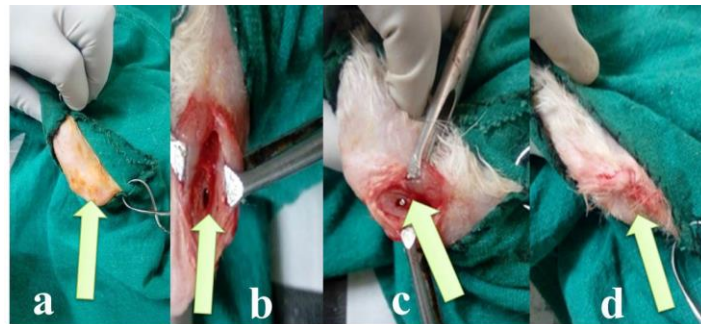


Figure 3.3: Surgery technique (a) Bone defect area (b)bone defect (c) implant placed in the bone defect (d) after stitching

3.2.12.4. Radiological examination: Radiographs were taken just after the operation, 30th day, and on 90th day postoperatively of the operated distal epiphysis femur bone for studying the position of the implant and host bone reaction to the implant.

3.2.12.5. Histological study: The nitinol implanted distal femoral epiphysis was collected on the day of sacrifice for histological analysis to check the cellular response of host bone to the implants. The implanted nitinol implants along with the surrounding bones were collected from the animals after sacrificing the animal. The bone pieces (3–4 mm thick) taken from implanted area were cut (3–4 mm thick) using a hacksaw. These bone specimens from adjacent bone at the side and at the bottom of the original bone defect were collected and washed thoroughly with normal saline and were fixed in 10% formalin for 7 days. All the specimens of bone tissue were decalcified using Goodling and Stewart's fluid(formic acid 15 mL, formalin 5 mL, and distilled water80 mL solution), followed by fixation with 4% paraformaldehyde. Finally, the decalcified bone tissues were embedded in paraffin wax for preparation of 4 μ m thick sections and stained with hematoxylin and eosin (HE). The

histological scoring method was adopted to calculate bone formation semi-quantitatively. A scale of 0–4 was taken to compare the cellular events with “0” indicative of absence, while “1–4” was for mild, moderate, marked, and severe, respectively. From each slide, three sites were examined by an assessor, and cross-examination was carried out by a blind observer.

3.2.12.6. Microstructural studies: The interface study of the bone and implant was verified by the detailed SEM study (JEOL JSM 5200 model, Tokyo, Japan). After removing the soft tissue, the implanted bone specimens were fixed in 5% glutaraldehyde phosphate solution followed by washing for 30 min with PBS (pH 7.4) and distilled water. The samples were then dehydrated in a series of graded alcohol solutions. Finally, the samples were dried with hexamethyldisilazane. A gold conductive coating was carried out by ion sputtering (JEOL ion sputter, Tokyo, Japan, model JFC1100, Japan) at 7–10 mA and 1–2 kV for 5 min for the

3.2.12.7. SEM study: The resin-mounted sample surfaces were then examined under SEM after proper alignment to assess the direction and orientation of newly formed bony tissues and distribution/absorption of materials at the defect site.

3.2.12.8. Oxytetracycline labelling study: The oxytetracycline labelling study was done to assess new bone formation. Fluorochrome (oxytetra cycline dehydrate;Pfizer India, Mumbai, India), at a dose of 25 mg/kg body weight, was given 3 weeks before the sacrifice of the samples of 30 day and 90 days in the 2–6–2 pattern, postoperatively for double-toning of new bone. The implanted segments of the bone were collected and transverse section (2–3 mm) thickness including the implanted area was cut with the help of a hacksaw. Un decalcified ground sections were prepared as described in Ref.[6] and the sections were ground to 20 μ m thickness using different grades of sand paper. The specimens were kept wet by dipping in water during the entire procedure. The specimens were observed under UV light with Leica DM2000 Bright, Leica Microsystems, Weztlar, Germany, phase contrast and a fluorescence microscope including Leicaqwin software to find out the amount and source of newly formed bone. The amount of new bone formation was calculated using Image J software. Using this software, We measured the area that was covered by golden yellow color. The investigation was performed by taking data from three images of each group.

3.2.12.9. Micro-computed tomography: In order to study the nature of the implant, host bone-implant interactions and the new bone formation, the post operated bone samples were analysed using micro-CT (Phoenix V|tome|xS, GE, Germany). All the bone samples were

completely dried at room temperature. The bone samples were scanned at a voltage of 85 kV and a current of 70 μ A, with a voxel size of 18 μ m. Time fraction was 500 ms per image with 1000 images in one complete rotation. The constructed 2D images were compiled to build 3D models using VG studio MAX 2.2 software (Volume Graphics, Germany).

The results obtained from different varieties of nitinol revealed lot of scatter as a function of parametric variation. to obtain meaningful data we used ANNOVA (One-Way). The same procedure was followed for different varieties of materials and different techniques to maintain uniformity.

References:

1. B D Cullity, Elements of X-ray diffraction, 2nd ed. Reading, MA: Addison-Wesley; (1978).
2. E Landi, A Tampieri, G Celotti, SSprio, Alkaline and alkaline-earth silicate glasses and glass-ceramics from municipal and industrial wastes. *J. Eur. Ceram. Soc.* 20, 2377, (2000).
3. I. Zhitomirsky, Cathodic electrodeposition of ceramic and organoceramic materials. Fundamental aspects, *Adv. Colloid Interface* 97, 279–317 (2002).
4. R. Ferrari, R. Moreno, EPD kinetics: a review, *J. Eur. Ceram. Soc.* 30, 1069–1078, (2010).
5. A. A.Green. The Preparation of Acetate and Phosphate Buffer Solutions of Known P_H and Ionic Strength, *Journal of the American Chemical Soceity*, 55 (6), 2331–2336, (1933).
6. S.K. Nandi, S.K. Ghosh B. Kundu, D.K. De, and D. Basu: Evaluation of new porous b-tri-calcium phosphate ceramic as bone substitute in goat model. *Small Rumin.Res.*75, 144 (2008).

CHAPTER 5:
RESULTS & DISCUSSIONS

Results and discussion chapter consists of different parts. It starts with the physical characterization followed by the results of chemical and subsequently in-vitro and in-vivo studies. FESEM and EDAX study of nitinol samples along with XPS, XRD, FTIR are reported first and then leaching study, wettability study, 3DProfilometry, cell culture and in-vivo study are reported one after another.

5.1. Physical Characterization of Bare and Silanized Nitinol:

5.1.1a. FESEM and EDAX Study of Bare Nitinol:

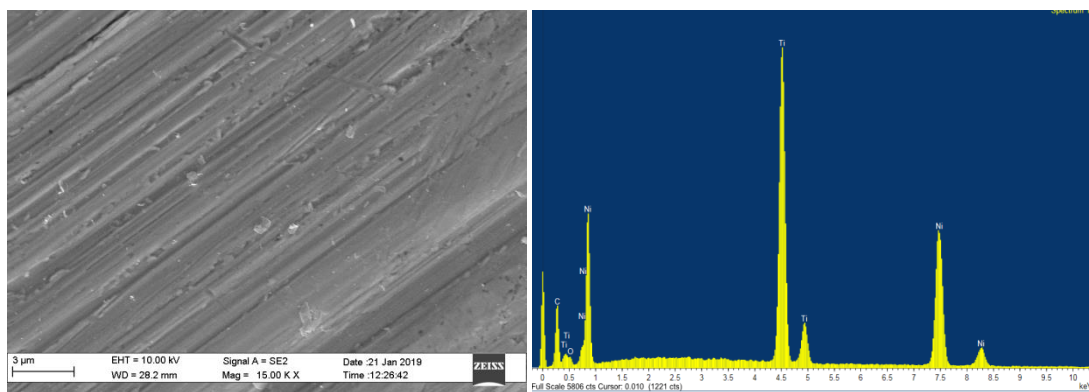


Figure 5.1a : FESEM and EDAX of Bare NiTi

Figure 5.1a shows the FESEM and EDAX study of Bare Nitinol. FESEM and EDAX study of supplier provided Bare Nitinol confirms to the composition of standard Nitinol, where the major peak of titanium and nickel was present. FESEM reveals lot of parallel striations which may be attributed to the mechanical polishing operation. Such uniform and parallel marks of polishing were observed in all specimens, observed under scanning electron microscope. Here we have presented a representative one.

5.1.1b. FESEM and EDAX Study of Silanized Nitinol:

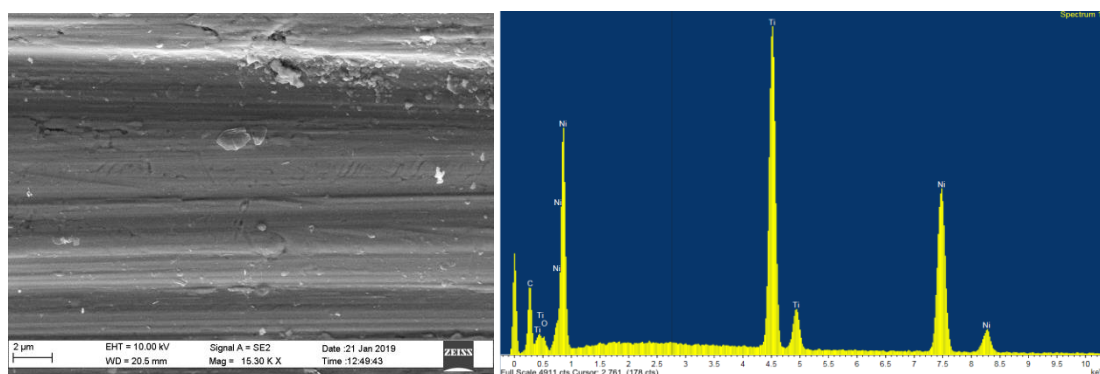


Figure 5.1b: FESEM and EDAX of Silanized Nitinol

Figure 5.1b shows the FESEM and EDAX study of Silanized Nitinol. EDAX study confirmed that the sample was Nitinol but EDAX study of Silanized sample did not show any peak of Si which was supposed to be the confirmatory peak of silanization. May be this happened due to the use of small percentage of APTES. That is why X-Ray photoelectron spectroscopy was done to get the evidence of silanisation. In FESEM of silanized surface no major change was observed in the basic texture however the application of APTES definitely added some new features in the form of patches or droplets on the nitinol surface.

5.1.2. XPS Study of Bare and Silanized Nitinol: The surface chemistry of bare and silanized nitinol has been studied by XPS. Figures 5.2(a) and 5.2(b) show the XPS spectra of bare and silanized nitinol. Bare Nitinol surface mainly consists of relatively thick layer of carbon and oxygen. The survey scan reveals that surface also consists of N, Cr, Fe, and Ni. The silanized surface shows the presence of Si2p which indicates the APTES immobilization on the surface of nitinol [Figure 5.2(c)]. This element was absent in the case of bare nitinol. The amount of C1s and O1s has been substantially increased, whereas the Ni1s is reduced in silanized surface compared to the bare nitinol.

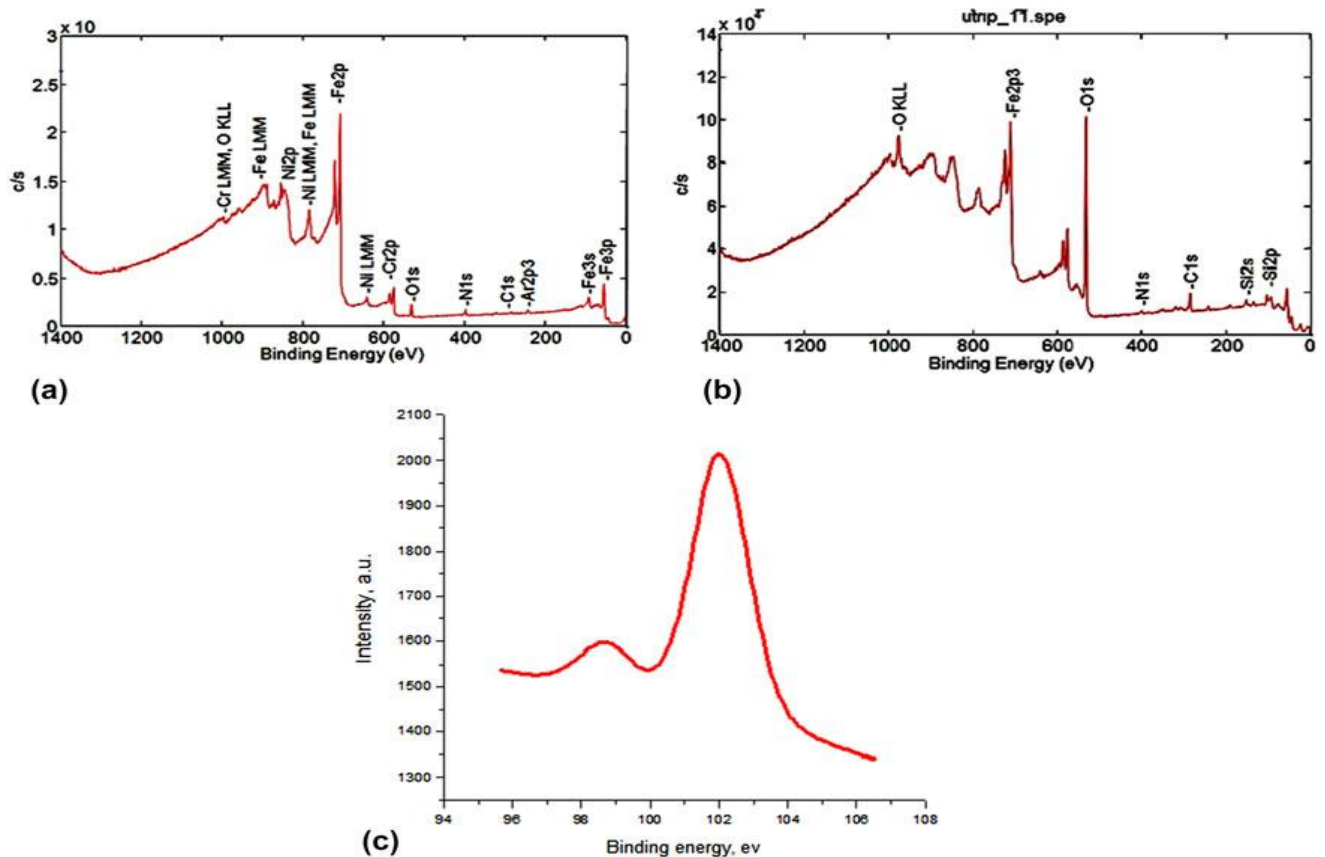


Figure 5.2: (a) XPS of bare nitinol; (b) XPS of silanized nitinol (showing the presence of Si); (c) Si2p spectra from the silanized sample.

5.2. Characterization of HAp powder:

5.2.1. XRD of Pure HAp:

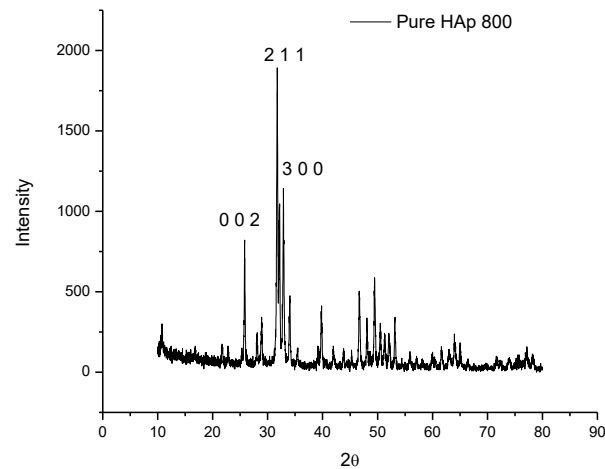


Figure 5.3: XRD of Pure HAp

The x ray diffraction of Pure HAp shown in figure 5.3. The major peak was found at 31.7° 2θ which is matched with the standard HAp JCPDS-ICDD powder diffraction file (PDF no. 09-0432). Minor amount of secondary phase α -TCP was also observed at 34.06° 2θ having PDF no.09-0348. The lattice parameter (a and c axis) and unit cell volume of the hexagonal structure of Hydroxyapatite calculated was calculated using standard formula and presented in table 5.1. The percentage of crystallinity was also calculated.

Table 5.1: Lattice parameter of calcined pure and doped HAp powder

Specimen	a axis	c axis	Unit cell volume	% of crystallinity	Crystallite size
Pure HAp	9.419 Å	6.898 Å	1584.4 Å ³	90.2	413 Å

The sharp peak of HAp confirms high value of crystallinity as well.

5.2.2. FTIR of Pure HAp:

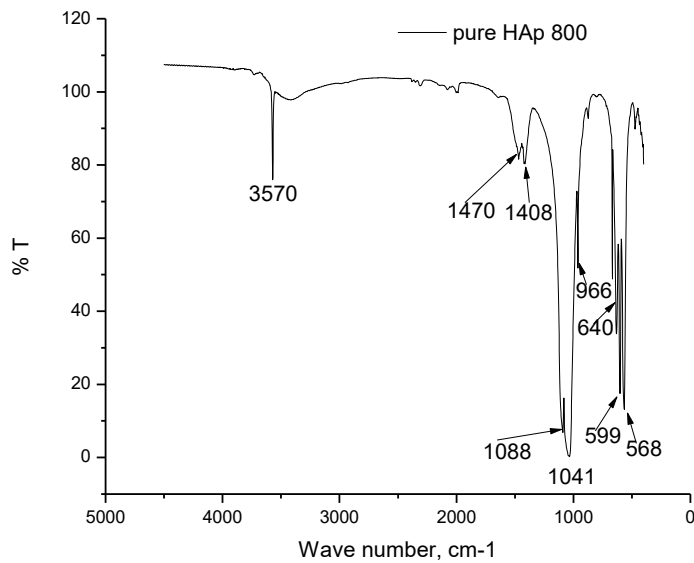


Figure 5.4: FTIR of Pure HAp

Figure 5.4 shows the FTIR spectra of pure HAp. The peak for Hydroxyl group appeared at 3570 cm⁻¹. The doublet appeared at about 568 cm⁻¹, 599 cm⁻¹ due to asymmetrical ν₄ stretching of PO₄³⁻ and band at 1041 cm⁻¹ was due to asymmetrical ν₃ stretching vibrations of PO₄³⁻, while the doublet at 1470 cm⁻¹ and 1408 cm⁻¹ arisen from CO₃²⁻. The phosphate ions of hydroxyapatite were found at 1088 cm⁻¹, 1041 cm⁻¹.

5.3. Characterization after Electrophoretic deposition:

5.3.1. FESEM of HAp Coated NiTi:

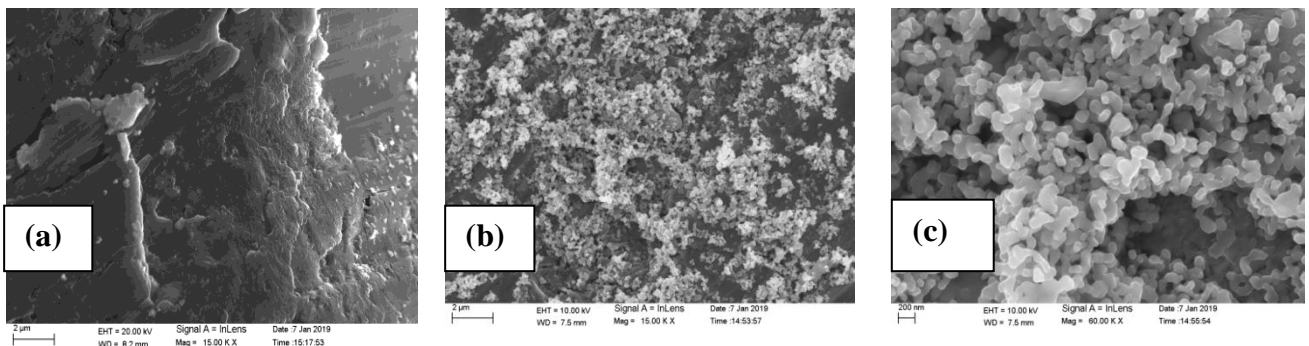


Figure 5.5a : FESEM of HAp Coated NiTi with layers structure and lot of porosity

Figure 5.5a showed that layer by layer Hap deposited on nitinol surface and it was not a uniform coating. Higher magnification reveals equiaxed grain of sub micron size . It is evident that HAp coating formed in layers (a) and the surface of the coating appears to be quite rough with lot of smaller deposits. It may further be noted that the extent of porosity and the size of pore (b,c) are often quite high. It can definitely add to the cell-material interaction which used in biological systems.

5.3.2. EDAX of HAp Coated NiTi:

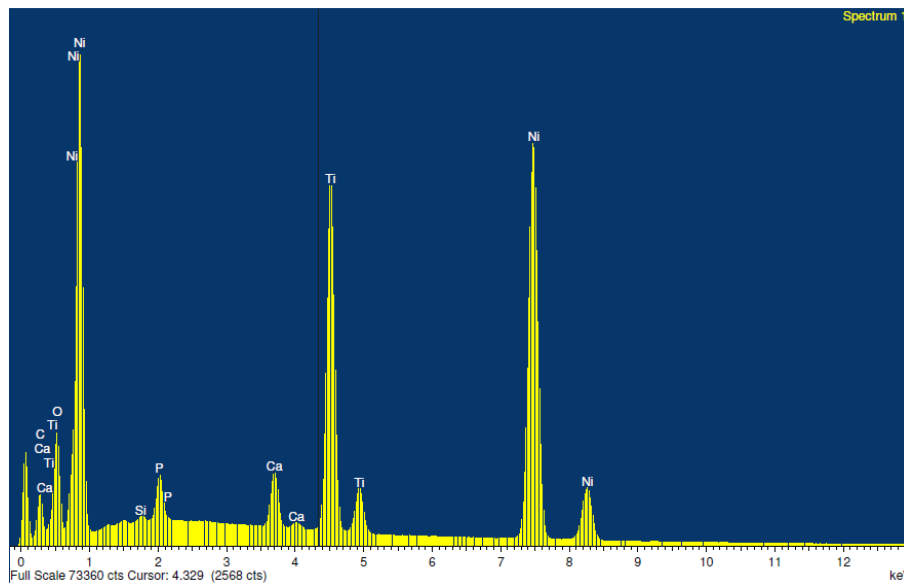


Figure 5.5b: EDAX of HAp Coated NiTi

From EDAX (figure 5.5b) study it was clear that coating of HAp by electrophoretic deposition was developed on Nitinol surface.

5.3.3.XRD of HAp powder scratched from the Coated NiTi:

Using Rigaku diffractometer, Ultima-III, Rigaku Co., Tokyo, Japan X-ray diffraction analysis was done on the deposited powder to check if there was any change in the form of hydroxyapatite after electrophoresis.

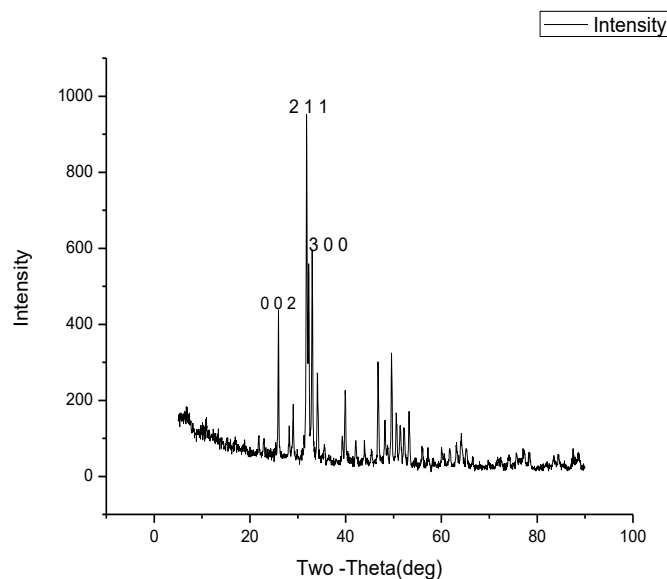


Figure 5.6: XRD of HAp powder scratched from the Coated NiTi

The x ray diffraction of scratched sample of coated material is shown in figure 5.6. The major peak was found at 31.7° 2θ which matched with the standard HAp JCPDS-ICDD powder diffraction file (PDF no. 09-0432). The other usually expected peaks are also observed. The sharpness of the signature peaks of the HAp denotes high level of crystallinity as well.

5.4. Leaching study: From the literature review it was evident that leaching is a major point of concern in case of nitinol but it is the quantum of leaching which is the most important issue. Daily dietary limit for nickel is 300–500 μg and here observed data is much lower than daily limit. Ni release from bare Nitinol and Coated Nitinol was more or less same for all the time intervals. But in case of Silanized Nitinol sample leaching of Ni is marginally more. Figure 5.7 shows the leaching characteristics over a span of 7days. It is clearly evident that silanization and coating did not have a effect on controlling nickel release. Here it may be noted that neither silanization nor coating through EPD could ensure that the whole surface is covered with a protective layer. It is already evident from XPS, SEM, EDAXA, and FESEM micrographs that new layers, deposits are there but lot of discontinuation are also existing. In fact these surface modifications perhaps debonds the inherently present protective oxide layer on Nitinol and creates holes, pits and discontinuities to cause corrosion and leaching of Ni^+ ions.

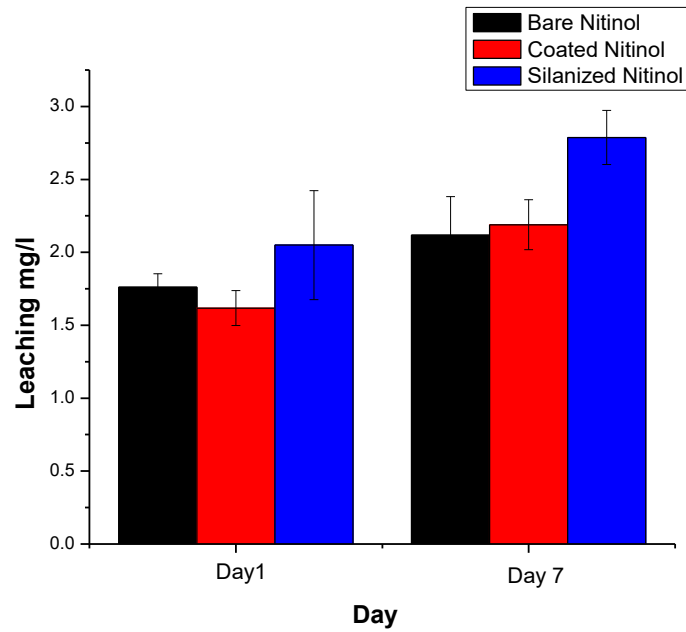


Figure 5.7: Ni⁺ leaching study over seven days

5.5. Wettability Study: For any material which is considered to be a prospective biomaterial, wettability is very important property. In this study wettability is not so pronounced. In all three varieties contact angles were more than seventy degree.

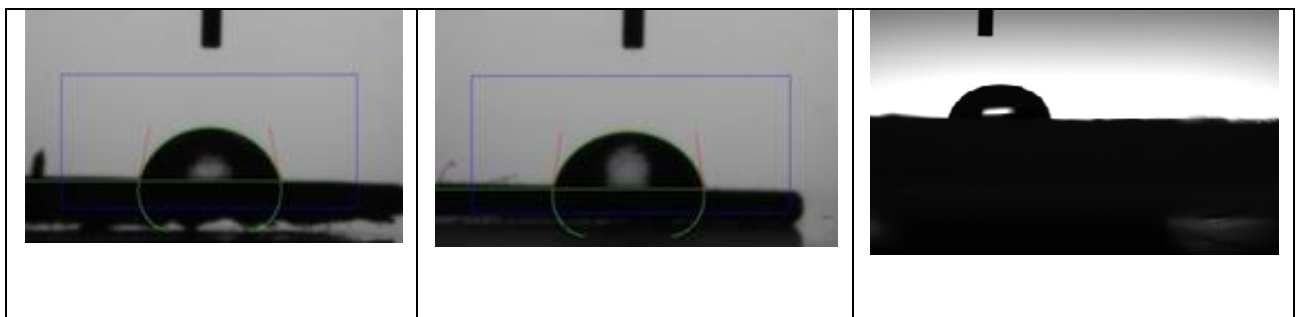


Figure 5.8. Contact angle of a) Bare Nitinol b) Silanized Nitinol c) Coated Nitinol

Table 5.2: Contact angle of (a) Bare Nitinol and (b) Silanized Nitinol

Sample	CA(M) [deg.]	t [sec]
Bare Nitinol	72.87	268.55
Silanized Nitinol	81.13	809.63
Coated Nitinol	73.3	32.9

CA(M) - Contact Angle Mean (in degree); t - Drop Age (in second)

Though there is no significant change in the contact angle of bare nitinol, silanized nitinol and coated nitinol but in all the cases wettability is good. This wettability will help cells to adhere on the surface of the substrate. During in-vivo study wettability may help to regenerate bone as well.

5.6. Roughness study:

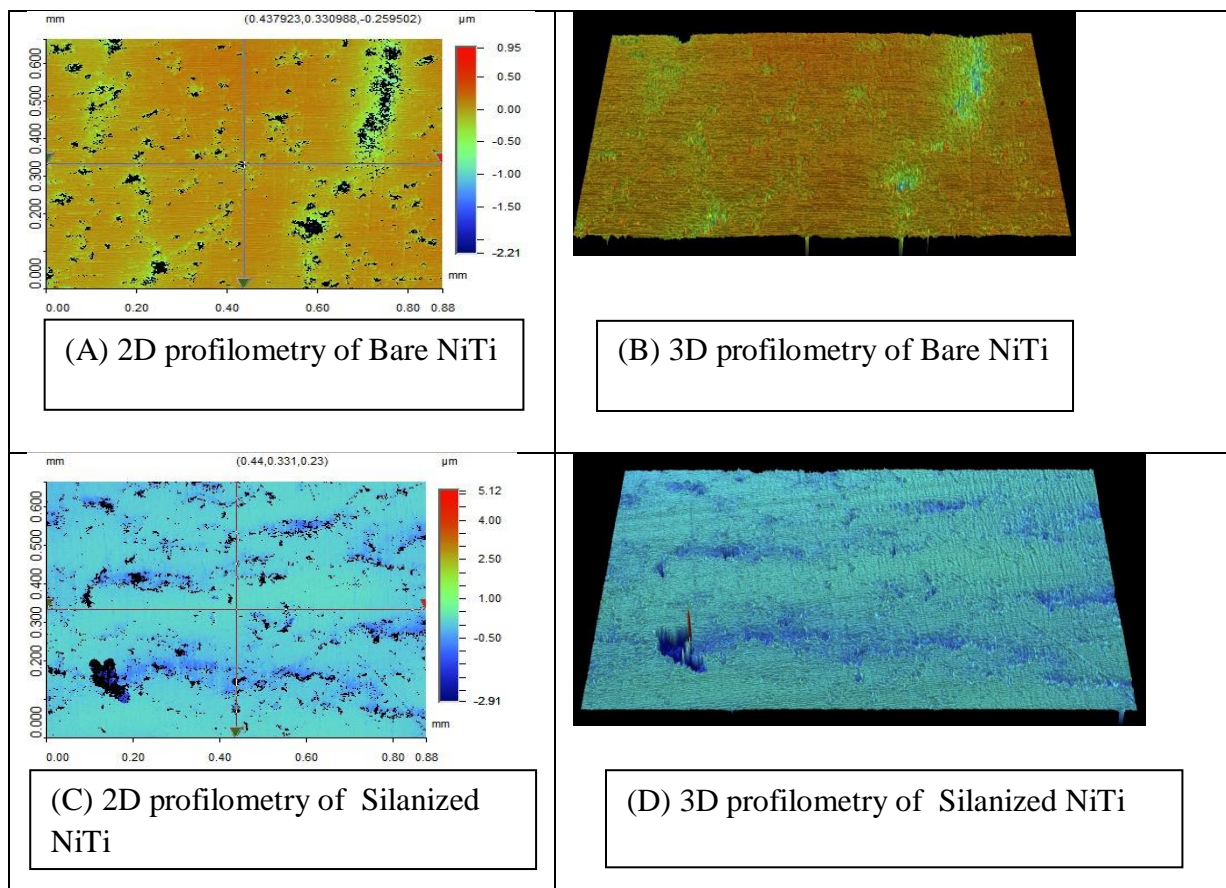


Figure 5.9: Surface roughness (A) 2D profile of Bare Nitinol (B) 3D profile of Bare Nitinol (C) 2D profile of Silanized Nitinol (D) 3D profile of Silanized Nitinol

Figure 5.9 shows the 2D and 3D surface roughness of Bare Nitinol and silanized Nitinol surface. From table 5.3 it was observed that in case of silanized Nitinol the centre line average (Ra) value was slightly high. Ra values denote that the surface was rough and it helped us to identify the effect of silanization on cell response. Rz value was calculated from the summation of height of the highest peak (Rp) and the lowest valley (Rv) contained by a single measuring length [1]. It was a little higher in silanized nitinol sample. It is expected that higher roughness will provide better support for the cells for proper anchorage. From the literature [2] it was also observed that the surface irregularities can be advantageous for anchorage for cells.

Though Ra values did not change much with silanization, it only provides an average data. In case of other parameters, it was evident that not only big peak value was there, the values corresponding to Rt and Rv are also higher in silanized samples. So it is likely that silanized samples provide more anchorage sites for the cells in case of cell-material interaction.

In case of coated Nitinol the same instrument was not available for measuring the roughness because of some technical problem, surface roughness of coated specimens was measured by a simple profilometer (Talysurf, Surtonic 3P) with identical cut off length and comparable traverse length. The results are shown in table 5.3. A simple comparison reveals that Ra value in coating was higher than that in case of silanized specimen or bare Nitinol. It conforms to the findings of FESEM.

Table 5.3: Surface roughness of (a) Bare Nitinol and (b) Silanized Nitinol

	Bare Nitinol	Silanized Nitinol	Coated Nitinol
Ra (μm)	0.09	0.142	0.56
Rq(μm)	0.13	0.21	0.96

5.7. Cell Culture study:

5.7.1. Phase contrast micrographs:

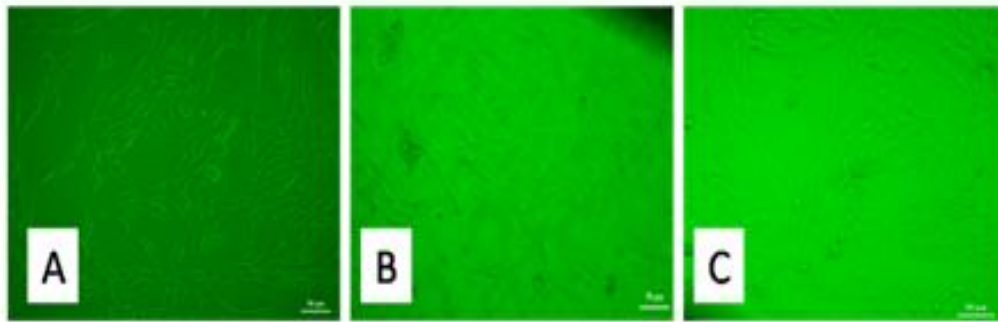


Figure 5.10: Phase contrast micrographs A) Control, B) Bare NiTi, C) Silanized NiTi

The micrographs of MG-63 cells harvested with bare and silanized nitinol samples [Figure 5.9 A, B, C] showed the live cells under the phase-contrast microscope. From these micrographs it is clearly noted that the cells were more or less in same condition in case of bare and silanized nitinol samples. No major difference could be observed.

5.7.2. Cell count:

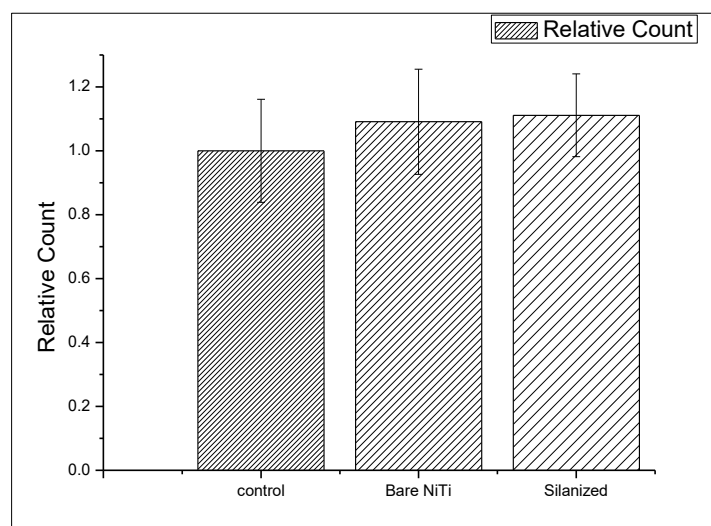


Figure 5.11: Cell count data of control, bare nitinol and silanized nitinol (48hours) (n=5)

Figure 5.11 showed the cell count data of control, bare nitinol samples and Silanized nitinol samples for 48 hours. Where Silanized nitinol samples showed slightly better proliferation

than bare nitinol. But Silanized samples showed high cell proliferation it may be attributed to the presence of Si which was definitely there on the surface (as evident from XPS).

5.7.3. MTT Assay: Part one:

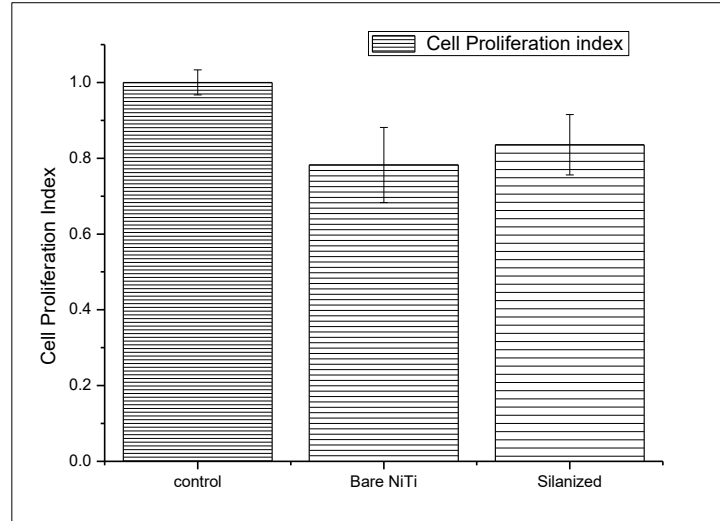
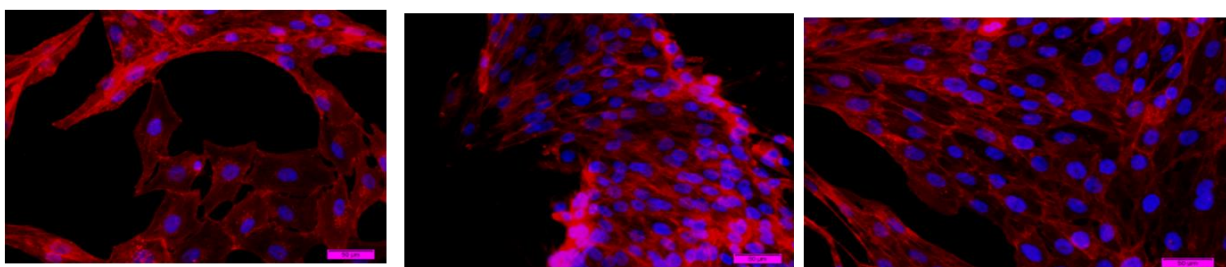


Figure 5.12: Cell proliferation data (48 hours) (n=3)

Figure 5.12 showed the proliferation data of bare nitinol samples and silanized samples for 48hours. Proliferation and differentiation of osteoblast are important in bone repair and regeneration. In this study, cell proliferation was checked by MTT assay. From literature it is known that incase of bare nitinol there is a high chance of toxicity as there is nickel present. Both the cases showed the same trend of proliferation. Silanized nitinol samples showed slightly better proliferation than bare nitinol.

5.7.4. Fluorescence micrography:



(a) Control

(b) Bare Nitinol

(c) Silanized Nitinol

Figure 5.13: Fluorescence micrographs: Here blue corresponds to (DAPI) and red (TRITC Phalloidin) corresponds to the nucleus and F-actin (a) Control (b) Bare NiTi (c) Silanized NiTi

The morphology of the adhered cells was examined under a fluorescence microscope. Fluorescence micrographs (figure 5.13) showed that after 24 hrs of adhesion, slightly more number of nucleus vis-a-vis cells were observed in case silanized samples. In none of the cases the cells seemed to be stressed, rather they were extending their filopods which denotes that the surfaces did not have any adverse effect on the osteoblast cells.

5.7.5. MTT Assay: Part Two:

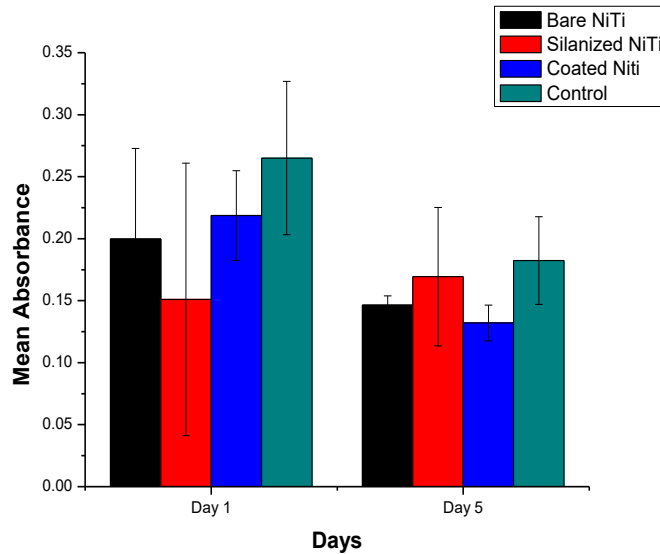


Figure 5.14: MTT assay analysis of control, bare nitinol, silanized nitinol and HAp coated nitinol

Figure 5.14 showed the proliferation data of bare nitinol samples, silanized samples and coated samples for 5 days. Though on day one control showed the best result but on 5th day silanized data showed best result followed by bare and coated nitinol samples.

5.7.6. 2D and 3D Confocal micrographs:

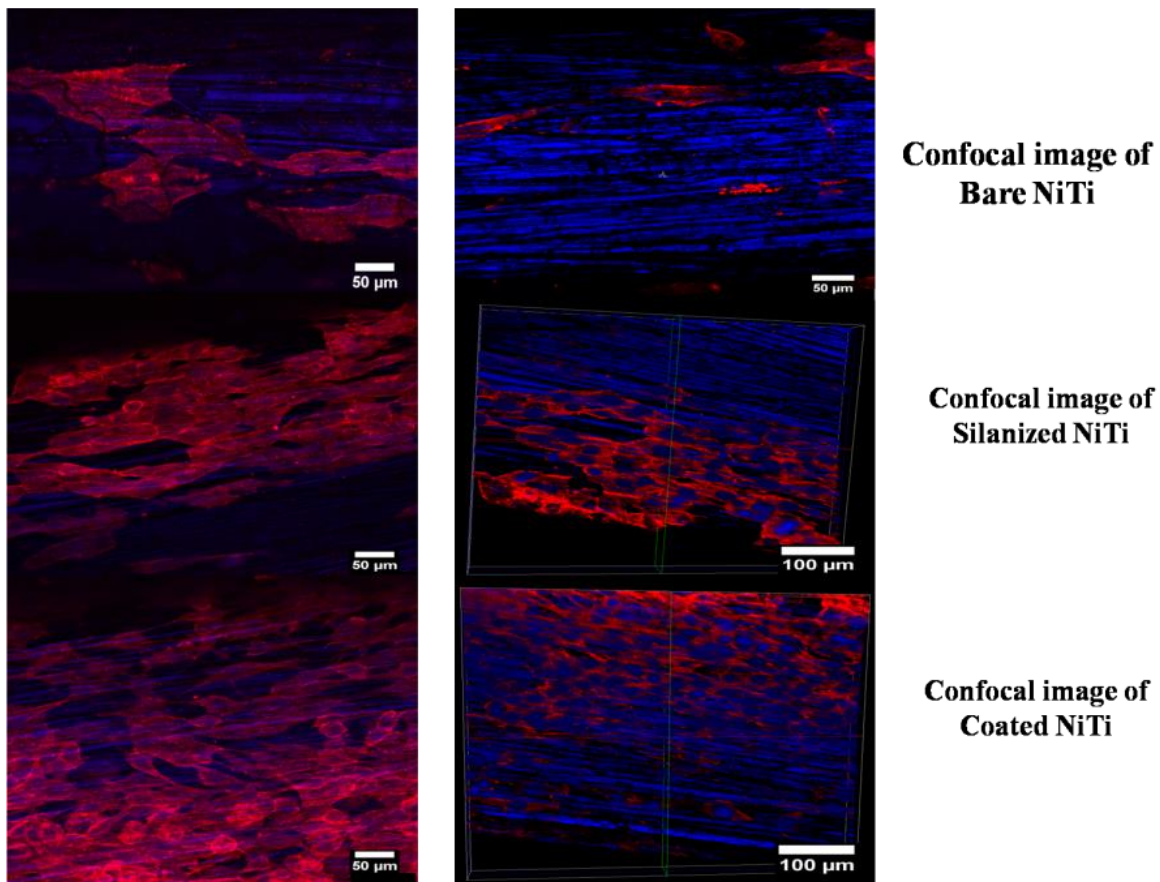


Figure 5.15: 2D and 3D Confocal micrographs of bare nitinol, silanized nitinol and coated nitinol samples

From 2D and 3D images it was found that in case of HAp coated Nitinol samples osteoblast cell growth was higher than silanized Nitinol followed by bare Nitinol samples respectively. Nucleus is clearly shown. From results of MTT assay in two parts, it is evident that cell proliferation in silanized specimens and coated specimens was better than bare nitinol due to presence of Si and HAp respectively. But out of these two varieties, it was difficult to locate the better one owing to their contradictory results observed in MTT assay and confocal images.

5.8. In-Vivo Study: In- vivo studies on healthy New Zealand rabbits over a span of one and three months postoperatively reveal lot of information through histopathology, radiology, flurochrome labeling, SEM and micro-CT(2D and 3D).

Histology Study:

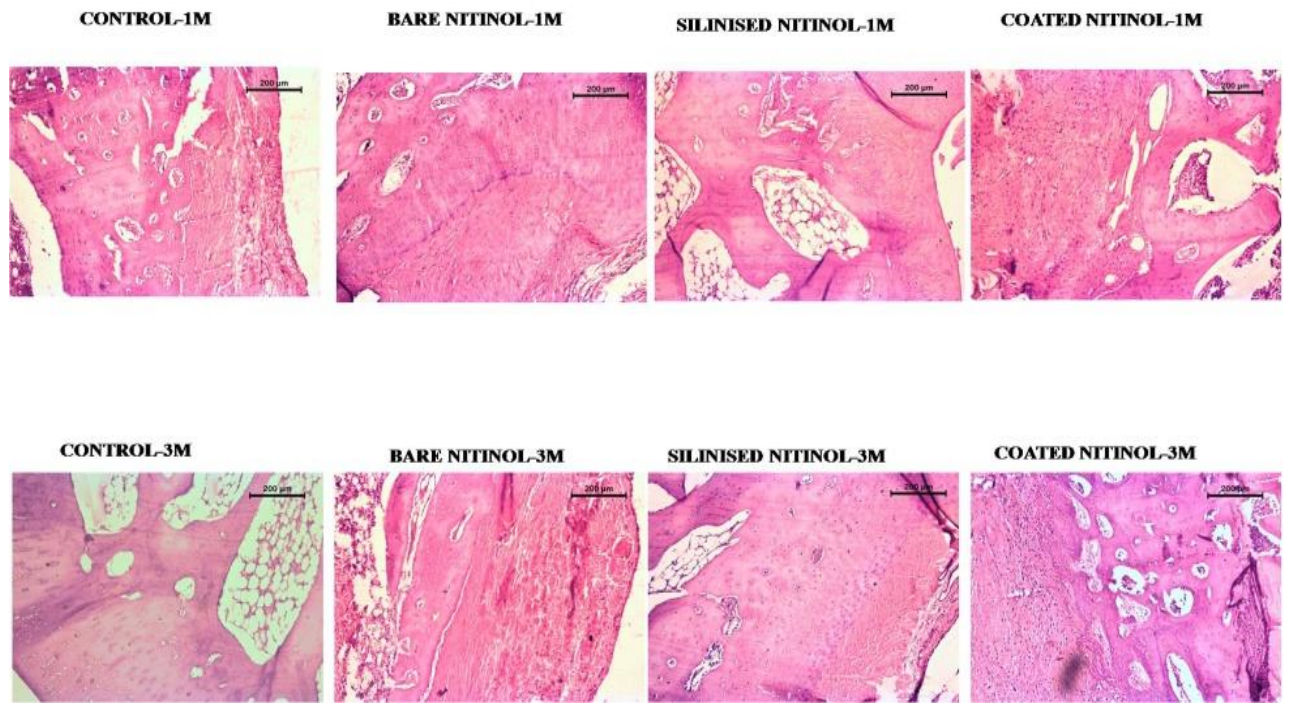


Figure 5.16: Hematoxylin and eosin (HE) stained histological images of Control sample section after one month, Bare Nitinol sample section after one month, Silanized Nitinol sample section after one month and Coated Nitinol sample section after one month Control sample section after three months, Bare Nitinol sample section after three months, Silanized Nitinol sample section after three months and coated Nitinol samples after three months

A detailed analysis of all the figures is presented below.

Control- one Month: The section depicted bony tissues along with perichondrium arranged orderly along with proliferation of few osteoblast and osteoclast. The osteocytes were well arranged and the medullary spaces contained fat cells, few osteoblast, R.B.C and scanty fibrinous deposit.

Control- three Months: The section showed a bony structure containing osteoblast and osteocytes. The Haversian canal was laid by fibrinous matrix and presence of few osteocytes around the lacunar spaces. The pericortical spaces contained fibro-cartilagenous structure invaded by few osteocytes.

Bare nitinol- one Month: The photomicrograph showed bony tissue with osteoclastic activity around the peri-medullar spaces. The medullary cavity contained abundant osteoblast, R.B.C and fibrinous exudate.

Bare nitinol- three Months: The photomicrograph showed bony structure consisting of abundant Haversian canal, sinusoidal space and few lacunae. The entire osteogenicstroma was embedded with abundant osteoclast, osteoblast in definite arranged manner. The medullary spaces were filled with few R.B.C, osteocytes and fibrinous exudate.

Silanized nitinol- one Month: The section depicted a bony structure consisting of few osteoblast and solitary osteoclastic activity. The medullary canal showed fat droplets, R.B.C's and scanty fibrinous exudate. Proliferation of osteoblast around the peri-cortical spaces as well as in medullary region was prominent.

Silanized nitinol- three Months: The photomicrograph showed solid osteogenic proliferation with presence of abundant osteoblast and osteoclast. The Haversian canal was well arranged and the lacunar spaces contained few osteocytes and fat cells. The medullary cavity contained scanty RBC and fibrinous deposit.

Coated nitinol -one Months: The photomicrograph depicted a newly formed bony osteoid containing multiple osteoblast and osteoclast. The peri-cortical spaces were rich in osteocytic cell, fibrinous exudate and abundant R.B.C. The lining area of medullary spaces was enriched with multiple osteocytes and Haversian canal.

Coated nitinol-three Months: The photomicrograph depicted well regenerated osteogenicstroma consisting of abundant osteoblast and osteoclast. The total osteoid was invaded by abundant vascular channels. The medullary cavity contained osteocytes, R.B.C and mild fibrinous deposit.

Radiology Study: After implantation radiographic plates are generated at stipulated intervals to monitor the condition of the nitinol wires, in all three varieties.



Figure 5.17: Radiological images of Control sample, Bare Nitinol sample, Silanized Nitinol sample and Coated Nitinol sample on 30th day and on 90th day

Control: The skiagram at day of implantation showed radiolucent defect at the distal epiphysis of femur. The defect was observed to be obliterated partially with newly grown bony tissue at 1 month. The cortical line was faintly visible discontinuous. After 3months, the gap was completely filled up with neo osteogenic tissue with cortical continuation. At this stage medullary cavity at the defect site was observed to be more radiolucent and incomplete remodelling.

Bare nitreinol: The radiograph at the day of implantation showed presence of radio dense implant filling the distal epiphysis of femur bone. At 1 month, there was evidence of implant occupying the defect without any perceptible change of radio density. Subsequently on 3month, the skiagram evidenced compactly anchored implant at the defect site and the cortical line had been tightly adhered with the exterior age of the implant indicating process of remodelling of the defect.

Silanized nitinol: At the day of implantation, the radiograph showed presence of radio-dense implant filling the distal epiphysis of femur bone. There was periosteal reaction around the exterior extremities of the implant at 1 month. At this time point, hyperdense newly formed bony tissue was observed partially obliterating the defect along the line of implant. Subsequently at 3 month, the skiagram showed complete continuity of cortical line at the defect site and compactly adhered implant within the medullary cavity. The radio density of the implant seemed to be unaltered indicating the advance stage of remodelling.

Coated nitinol: The skiagram at the day of implantation showed presence of tightly packed implant touching the interior extremity of the trans cortex. At 1 month, the radiograph showed compactly adhered implant at the defect with well defined thick cortical line adjacent to the defect, the implant seemed to be radiologically unaltered in term of size, shape and density. Finally at 3 month, complete obliteration of defect was noticed with continuous cortical line of similar radiological features to that of adjacent host site. The implant was noticed within the medullary cavity without alteration of density, size and shape.

Fluorochrome labelling study: The photomicrograph of the fluorochrome studies of control group at one month depicted bright golden yellow fluorescence of newly formed bony tissue (28.33%) at the centre of sea green backdrop. At the same time point, the bare nitinol group showed more formation of newly formed bony tissue (38.43%) as bright golden fluorescence as compared to control one. The Silanized bone photomicrograph showed abundance of golden yellow fluorescence (50.61%) in more regions. The coated nitinol bone samples at this time point also showed more region (52.71%) of golden yellow fluorescence in the background of deep sea green coloured host tissue indicating more bone formation. At three month, the photomicrograph of control sample of interval showed moderate golden yellow fluorescence of osseous tissue (33.21%) in a scattered zone. The golden yellow fluorescence of newly bony tissue (50.79%) was observed throughout the section in bare nitinol sample. The Silanized nitinol group showed wide area (71.26%) of golden yellow fluorescence as compared to its earlier time point indicating active state of bone regeneration. Finally, the coated nitinol group showed more golden yellow fluorescence in a wide region in the background of deep green sea coloured host tissue (73.33%).

It appears once again (after the results and discussion on MTT-assay) that the performances of coated and silanized specimens are comparable after three months. So it is really tough to decide the better among the two options but a careful examination of one month data clearly suggests that coated samples promoted new bone formation faster than silanized samples. As it is a semi quantitative analysis rather than a quantitative estimation, this point of superiority of coating over silanized variety may be noted.

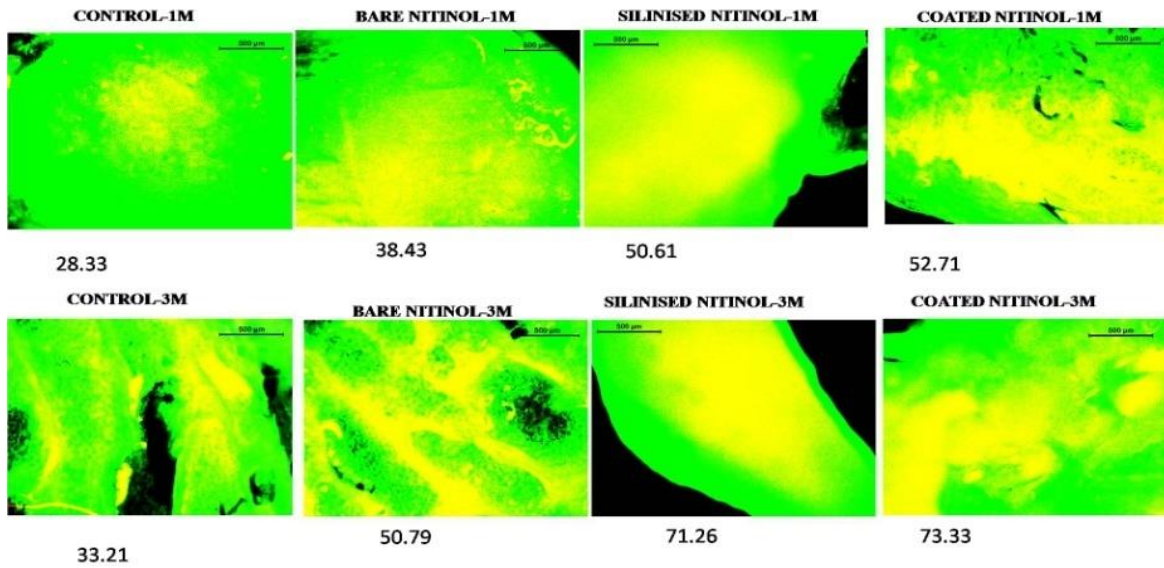


Figure 5.18: Fluorochrome labelling image of Control sample after one month and three months, Bare Nitinol sample after one month and three months, silanized Nitinol sample after 1month and 3months, Coated Nitinol sample after 1month and 3months . Host / old bone (green portion) and new bone (yellow portion , shown in percentage as well)

Microsturctural study:

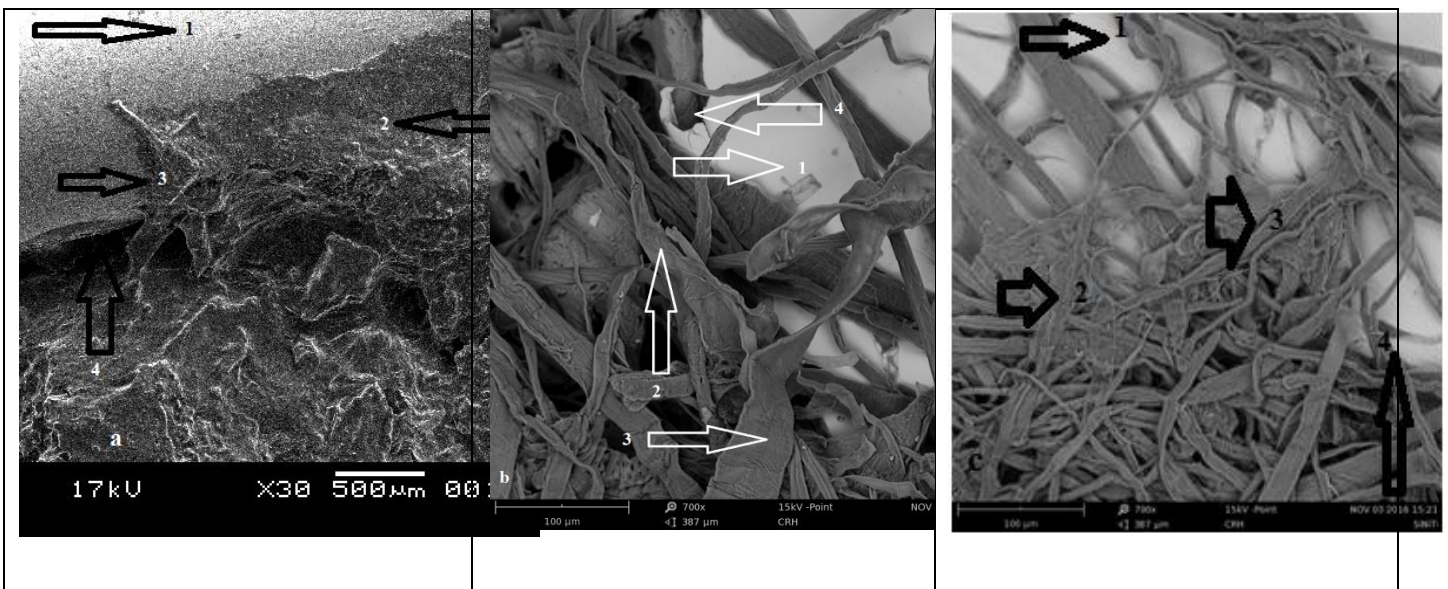


Figure 5.19:SEM micrographs of (a) Bare Nitinol sample of 30days (b) Silanized Nitinol of 30 days (c) Coated Nitinol sample of 30days (1 denotes Nitinol implant,2 denotes tissue 3 denotes tissue growth over the implant 4 denotes the shortened gap between the implant and bone tissue)

Figure-5.19 shows the SEM micrographs of host bone implant interface region after one and three months postoperatively. New tissue formation over the implant was observed for all specimens. But it was clearly evident that new bone tissues bridged the interface of bone-implant more readily and more effectively in silanized sample. Even after 30 days, there was still some gap between the bare nitinol implant and the host bone which was not there in case of silanized specimen. In fact the figures clearly denote how the new tissue formation gradually filled the gap and continued to spread and grow over the implant surface.

One of the possible reasons behind the high growth rate of new bone formation in silanized Nitinol, as evident from almost all the studies mentioned above, is the incorporation of Silicon thorough the silanization process. From literature it is evident that Silicon is involved in the collagen matrix formation as well as bone mineralization. Silicon is not a part of these tissues, but instead acts as a catalyst in the processes. Researchers have established that Silicon plays a crucial role in inter- and intra-cellular signaling pathways and hinder osteoclast formation vis-a-vis bone resorption. Silicon has the property to bind with glycosaminoglycans and helps in the formation of cross-links between collagen and proteoglycans. From in-vitro studies it has been found that silicon stimulates type1 collagen synthesis and osteoblast differentiation. The exact progression of mineralization is not known, but silicon plays a vital role to make the bone matrix more calcifiable. To maintain the bone strength, Silica and calcium work together. Silica has the unique ability to “make the most” of available calcium, almost amplifying its effects in building bone. Consequently it triggers calcification process for new osseous tissue deposition. It also improves bone matrix quality and facilitates bone mineralization, so it’s not surprising that fracture healing rates increase in the presence of silica, even if calcium is relatively low [3-11].

The marked superiority of silanized samples may be attributed to this however further study with detailed cell-material interaction is needed before final conclusion. However one thing is clearly evident that mere silanization of nitinol can definitely offer some specific advantages in terms of reducing leaching or promoting osseous bonding. In case of coating similar patterns of tissue growth over the coated nitinol specimens were observed [Figure 5.19c] but no marked difference was there.

Micro-computed tomography: The *in vivo* bone regeneration and the bone-material interaction of all the bone samples were analyzed using micro-computed tomography and the 2D and 3D images are shown in figure 5.20 and figure 5.21. The 2D micro-CT images of

control, bare, silanized and HAp coated nitinol of 1month (1M) and 3 month(3M) are shown in Figure 5.20. The 1M post implanted 2D micro-CT images of bare, silanized and HAp coated nitinol showed characteristic irregular new bone regeneration around the implant material whereas, the control samples showed no onset of bony tissue formation. The 90 days post operated 2D radiographs of silanized nitinol showed complete closure of the defect site and higher amount of bony tissue (shown by red arrow) fully covering the implant material followed by HAp coated and bare nitinol. It may be attributed to the released Si ions compared to other samples. This released Si ions played a significant role in enhancing the bone regeneration

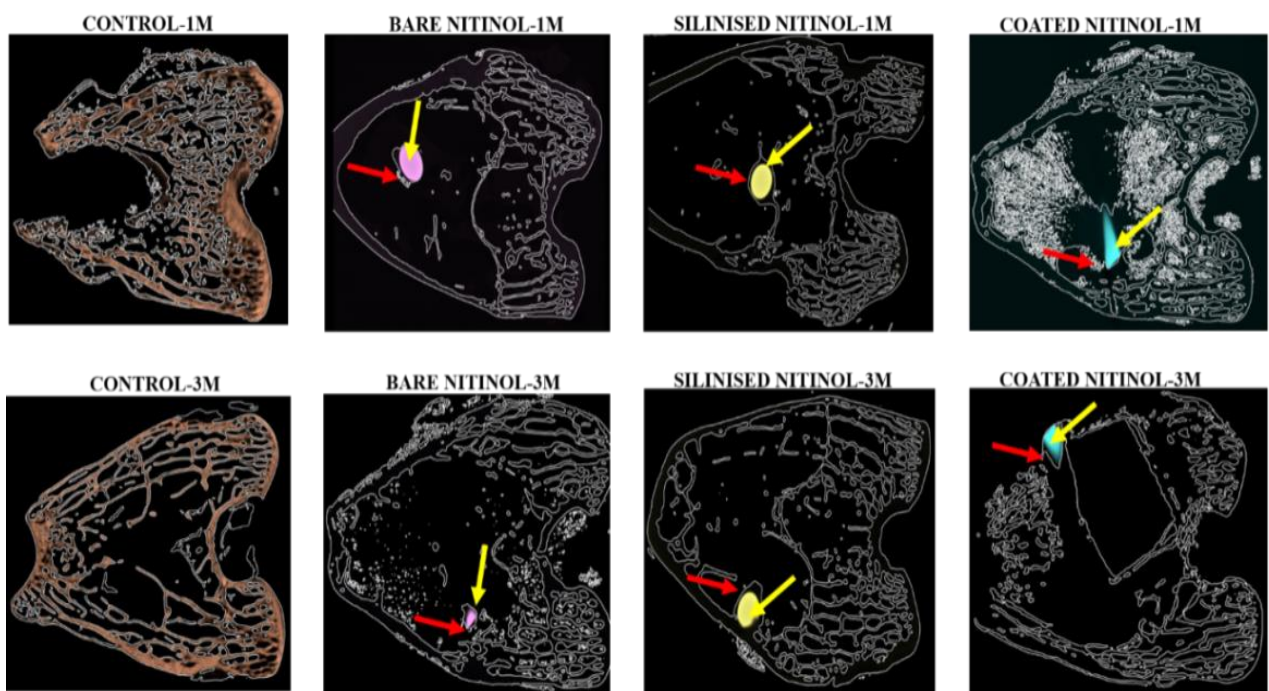


Figure 5.20: Radiographic 2D images of defect bone sites showing extent of healing after 1month and 3 month (Red arrow showing new bone growth around the implant; yellow arrow showing implant material)

The 30 days 3D images (Figure 5.21) of bare, silanized and HAp coated nitinol showed that the implanted samples showed that bone has started to grow on all the implants indicating the osteoconductive nature of the material. With increasing time from 30 to 90 days, partial bone accumulation are seen inside and around the defect area for bare and Hap coated nitinol whereas, silanized nitinol showed finer and matured bone formation completely filling the defect hole showing the complete formation of periosteum (Figure 5.21).The resorption process was more pronounced for silanized nitinol with thick newly formed bony tissue and

large struts of trabecular bone were formed on the implant. The enhanced bone growth for silanized nitinol may be due to the positive effect of Silicon.

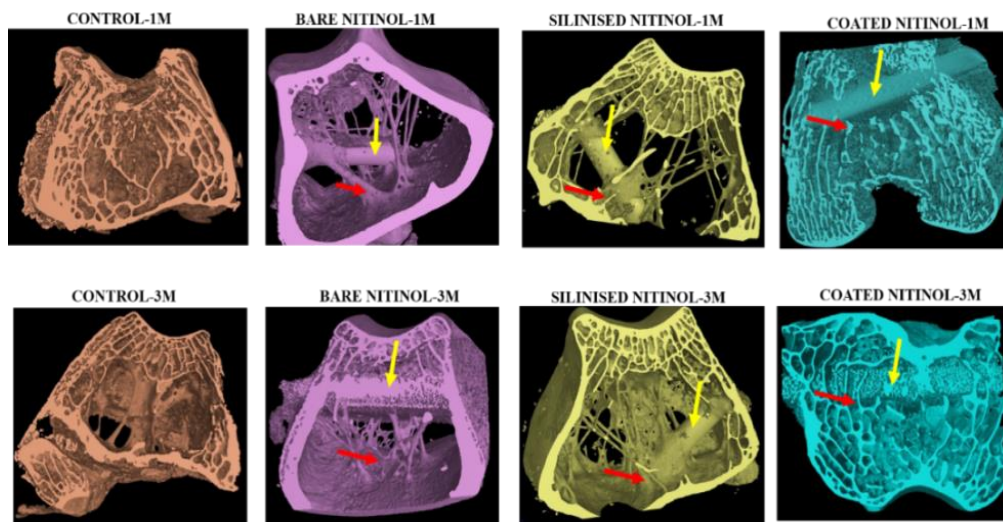


Figure 5.21: Radiographic 3D images of defect bone sites showing extent of healing after 1 month and 3 month (Red arrow showing new bone growth around the implant; yellow arrow showing implant material)

For any successful clinical application of an implant, the *in vivo* bone regeneration property is an essential prerequisite. Based on the fruitful results of *in vitro* we have implanted bare, silanized and HAp coated nitinol in distal femurs of rabbits. After 1M and 3M, all the bone samples were harvested and scanned using micro-CT for detailed bone growth with respect to time. The 1M 3D images showed the healing as well as the new bone formation around the implant materials. A comparative examination suggests that in silanized sample there was a closely knit bony tissue structure around the foreign material. It was so dense that the specimen could hardly be noticed. In that case the periosteum was completely formed with uniform thickness and there was clear sign of growing natural bone tissue. The sufficient amount of released Si ions played a significant role in enhancing the bone regeneration [12]. The released Si ions got embedded inside the nearby bony tissue served as a stimulant for bone marrow stromal cell differentiation and osteoblastic proliferation which resulted in the complete formation of periosteum [13]. Similar studies of Kim et al. also showed that the released Si ions from Si doped HA resulted in enhanced bone growth and faster healing of defect site in rabbit model [14]. Moreover, Si is important in elevating the synthesis of collagen type 1 and osteoblast differentiation and it also helps in early bone repair at the defect site [15].

Major Observations: Depending on all the results presented so far , following important and major observations can be made.

Silanization added Si to the surface of Nitinol however the layer was discontinuous as evident from subsequent results. EPD technique could deposit a sub-mm HAp containing on Nitinol though the coating was non-uniform.

Ni release from bare Nitinol and Coated Nitinol was more or less same for all the time intervals. But in case of Silanized Nitinol it is little bit more than other two.

From roughness: In case of coated and silanized Nitinol the centre line average (Ra) value were slightly high. Ra values denote that the surfaces were rough and it helped us to identify the effect of coating and silanization on cell response. It is likely that silanized samples provide more anchorage sites for the cells in case of cell-material interaction.

From Contact angle: There is no significant change in the contact angle of bare Nitinol, silanized Nitinol and coated nitinol but in all the cases wettability is reasonably good.

From MTT assay: In case of 48hours study of bare Nitinol and silanized nitinol Cell count data, Cell proliferation data and fluroescence micrographs clearly showed that silanized nitinol samples are slightly better than bare nitinol samples.

When details study was done with bare nitinol, silanized nitinol and HAp coated nitinol over a span of 5days, on day one control showed the best result but on 5thsilanized data showed best result.

From confocal study: From 2D and 3D images it was found that in case of HAp coated Nitinol samples osteoblast cell growth was higher than silanized Nitinol followed by bare Nitinol samples respectively.

From Histopathology of bone: The photomicrographs of bare Nitinol, silanized Nitinol and coated Nitinol samples showed proliferation with presence of abundant osteoblast and osteoclast. The Haversian canal was well arranged and the lacunar spaces contained few osteocytes and fat cells. The medullary cavity contained scanty RBC and fibrinous deposit.

Radilogy study: In all three samples formation of complete continuous cortical line at the defect site and compactly adhered implant within the medullary cavity were shown. The radiodensity of the implant seemed to be unaltered indicating the advance stage of remodelling.

Fluorochrome study: 1M and 3M Study showed that in case of coated Nitinol sample newly formed bony tissue growth rate is more comparable to silanized nitinol sample but much higher than to bare nitinol samples.

Scanning electro micrographs: SEM micrographs of host bone implant interface region after one and three months postoperatively, showed that new tissue formation over the implant was observed for all specimens. But it was clearly evident that new bone tissues bridged the interface of bone-implant more readily and more effectively in silanized sample and coated sample than bare.

From Micro CT study : From 2D micro-CT images of control, bare, silanized and Hap coated nitinol of 1M and 3M , 1M 2D images showed the healing as well as the new bone growth around the implant materials. The 90 days post-operated 2D radiographs of silanized nitinol showed complete closure of the defect site and the new bone regeneration around the implant. The 30 days 3D images showed that the implanted samples showed that bone has started to grow on all the implants indicating the osteoconductive nature of the material. With increasing in time from 30 to 90 days, partial bone accumulation are seen inside and around the defect area for bare and Hap coated nitinol whereas, silanized nitinol showed finer and matured bone formation completely filling the defect hole showing the complete formation of uniform periosteum

We have performed various experiments. From those qualitative and quantitative studies it was found that in some of the cases silanized nitinol showed better performance in in-vitro and in-vivo studies than the other two samples, while coated samples performed better in some other cases. In case of few important studies like Fluorochrome study which showed the quantity of new bone formed and Micro CT image which showed the pattern and formation of the bone cell and structure, both coated and silanized sample performed very well. MTT assay showed better performance of silanized nitinol and confocal images showed that cell proliferation rate was better in coated nitinol than other samples.

Further in depth studies involving silanized nitinol and coated nitinol samples are needed to understand the extent of superiority of one category over the other specimens in a more comprehensive way.

Table 5.4 : Comparison at a glance

Qualitative				Quantitative			
	Bare Nitinol	Silanized Nitinol	Coated Nitinol		Bare Nitinol	Silanized Nitinol	Coated Nitinol
In-Vitro							
				Leaching	Reference (1)	Poor (0.714)	Poor (0.9)
Confocal image study	Reference	Slightly better	Slightly Better	MTT assay	Reference (1)	Slightly Better(1.2)	Poor (0.9)
In-Vivo							
Histopathology of bone	Reference	Good	Good	Fluorochrome study	Reference (1)	Much better (1.4)	Much Better (1.43)
Micro CT image study	Reference	Much Better	Slightly better				

To make an effective comparison a comparative chart is prepared with both qualitative and quantitative data base and it was tried to non-dimensionalise the quantitative data for comparing. It reveals that in number of important domains, silanized samples performed slightly better than the other variety (Coated) . Only in case of mico-CT, silanized samples performed much better over a long time period. Hence it is proposed here to be the better option.

The results suggests that in case of in-vitro and in-vivo tests no specific variety of nitinol is uniformly better than others even in case of in-vitro results the superiority of one variety changed with time. In in-vivo study also results from different tests can lead to different conclusions. Consequently we had to take the help of existing literature [9, 12-15] as well as statistical analysis of important parameters to identify the most suitable variety or the variety with a higher number of superiority domains.

References:

1. Costa-Rodrigues J. , Fernandes A., Lopes M. and Fernandes M., *Acta Biomater.* 8, 1137–45 (2012).
2. Chanda A., Singha Roy A., Xue W., Bose S. and Bandyopadhyay A. , *Mater. Sci. Engg. C.* 29 1201-06 (2007).
3. Beck R. G., Ha W. S., Camalier E.C., Yamaguchi M., Li,J.K. Lee Y., and Weitzmann: N. M., Bioactive silica-based nanoparticles stimulate bone-forming osteoblasts, suppress boneresorbing osteoclasts, and enhance bone mineral density in vivo. *Nanomed.: Nanotechnol. Biol. Med.* 8, 793 (2012).
4. Carlisle M.E.: In vivo requirement for silicon in articular cartilage and connective tissue formation in the chick. *J. Nutr.* 106, 478 (1976).
5. Carlisle M.E: Silicon: A requirement in bone formation independent of vitamin D1. *Calcif. Tissue Int.* 33, 27 (1981).
6. Carlisle M.E: Silicon as an essential trace element in animal nutrition. *Silicon Biochem.* 703, 123 (2008).
7. Jugdaoh singh R.: Silicon and bone health. *J. Nutr. Health Aging* 11, 99 (2007).
8. Mladenovi Z., Johansson A., Willman B., Shahabi K., Björn E., and Ransjö M.: Soluble silica inhibits osteoclast formation and boneresorption in vitro. *Acta Biomater.* 10, 406 (2014).
9. Price T. C., Koval J.K., and Langford R.J.: Silicon: A review of its potential role in prevention and treatment of postmenopausal osteoporosis. *Int. J. Endocrinol.* 2013, 1 (2013).
10. Reffitt M. D., Ogston N., Jugdaoh singh R., Cheung H.F.J., Evans B.A.J., Thompson R.P.H, Powell J.J., and Hampson G.N.: Orthosilicic acid stimulates collagen type 1 synthesis and osteoblastic differentiation in human osteoblast-like cells in vitro. *Bone* 32, 127 (2003).
11. Schwarz K.: A bound form of silicon in glycosaminoglycans and polyuronides. *Proc. Natl. Acad. Sci. U. S. A.* 70, 1608 (1973).
12. Bavya Devi K., Tripathy B., Roy D.M. A., Lee B., Prashant N., Nandi K. S. and Roy M., “In Vitro biodegradation and In Vivo Biocompatibility of forsterite bio-ceramics: Effects of strontium substitution:”, *ACS Biomaterials Science and Engineering*, Vol. 05, pp. 530-543, (2018).
13. Hing A. K., Revell, P.A. Smith N., Buckland T., Effect of Silicon Level on Rate, Quality and Progression of Bone Healing within

Silicate-Substituted Porous Hydroxyapatite Scaffolds. *Biomaterials*, 27 (29), 5014–5026 (2006).

14. Shi M., Zhou Y. , Shao J., Chen Z., Song B., Chang J., Wu C., Xiao Y. Stimulation of Osteogenesis and Angiogenesis of HBMSCs by Delivering Si Ions and Functional Drug from Mesoporous Silica Nanospheres. *Acta Biomater.* 21 (Suppl. C), 178–189 (2015).

15. Kim S. B., Yang S. S, Yoon J. H., Lee j. , Enhanced Bone Regeneration by Silicon-Substituted Hydroxyapatite Derived from Cuttlefish Bone. *Clin. Oral Implants Res.* 28 (1), 49–56 (2017).

CHAPTER 6:
CONCLUSION & FUTURE
SCOPE

Conclusion

Current study involved silanization of bare Nitinol surface using APTES and also involved electrophoretic deposition of pure hydroxyapatite on bare nitinol surface where hydroxyapatite was synthesized by wet chemical process. Coating process by electrophoretic deposition was thoroughly optimized. Then the bare nitinol samples, silanized nitinol samples and electrophoretically coated hydroxyapatite nitinol samples were characterized for physical, chemical and detailed biological study.

Different results obtained from the existing study lead to the following major observations in brief.

- Presence of Si2p and Si2s X-ray photoelectron (XPS) spectra in silanized sample confirms the efficacy of the silanization process.
- Major peak in sintered hydroxyapatite specimen synthesized using wet chemical method has pure standard hydroxyapatite peak as observed from X-ray diffraction (XRD) analysis.
- The lattice parameter, crystallite size and high percentage (>90%) of crystallinity was also observed as pure hydroxyapatite.
- From the Fourier transformed infrared spectroscopy(FTIR) study, it was observed that it was pure hydroxyapatite powder consisting of standard hydroxyapatite peak.
- For electrophoretic deposition technique both the NiTi electrodes were placed parallel to each other within a distance of 15 mm and connected to the power supply where voltage for this work was 60volts and deposition time was 90 minutes with number intermittent drying after every 10 minutes. After deposition, the green coatings were dried with normal dryer for few minutes and after getting the desired coating the samples were finally dried at 80°C for 2 hrs.
- The X-ray diffraction of scratched sample of electrophoretically coated material has the major peak which matched with that of standard Hydroxyapatite.
- Ni release from bare Nitinol and Coated Nitinol was more or less same for all the time intervals. But in case of Silanized Nitinol it was little bit more than other two.
- Roughness values for bare, silanized and coated samples were widely different with Ra values 0.09 μm , 0.142 μm and 0.56 μm respectively.
- There is no significant change in the contact angle of bare Nitinol, silanized Nitinol and coated Nitinol but in all the cases wettability is good.

- In-vitro cell culture using MG63 osteoblast cells for a span of 5days showed that cell proliferation (MTT assay) was best result in case of silanized Nitinol specimen followed by bare and coated nitinol samples.
- But 2D and 3D confocal laser microscopic images showed that in case of HAp coated Nitinol samples osteoblast cell growth was higher than silanized Nitinol followed by bare Nitinol samples respectively.
- In-vivo characterization for one and three months revealed that no marked inflammatory reactions occurred in bare nitinol samples, silanized nitinol samples and hydroxyapatite coated nitinol samples.
- SEM study showed that the bonding of Silanized nitinol implants with bone was better than bare nitinol samples.
- Histopathology study revealed the presence and formation of haversian canals, lacunar spaces, peri-cortical spaces, vascular channels etc in all three samples .
- Oxytetracycline labelling study revealed that in case of coated Nitinol sample newly formed bony tissue growth rate is much more comparable to silanized nitinol sample but much higher than bare nitinol samples.
- Radiological study revealed that in all three samples formation of complete continuous cortical line was there at the defect site and compactly adhered implant within the medullary cavity were shown. The radio density of the implant seemed to be unaltered indicating the advance stage of remodelling.
- Micro CT study revealed that 2D micro-CT images of control, bare, silanized and Hap coated nitinol of 1M and 3M showed the healing as well as the new bone growth around the implant materials. With increase in time from 30 to 90 days, 3D images showed that partial bone accumulation are seen inside and around the defect area for bare and Hap coated nitinol whereas silanized nitinol showed finer and matured bone formation completely filling the defect hole showing the complete formation of periosteum.

Finally it may be concluded from various qualitative and quantitative studies that in most of the cases silanized nitinol showed better performance in in-vitro and in-vivo studies than the other two samples though silanized nitinol has slightly higher Ni⁺ leaching than other two but well within dietary limit. So, silanization on nitinol as a biofunctionalisation technique is a potential and viable option. But further detailed and controlled studies are required before going for a systematic clinical trial.

Future scope of the work:

- Improvement of the adhesion of the coating to the substrate.
- Study the effect of using other coating processes.
- Detailed cell culture study.
- In-Vivo study of the behavior of the surface modified nitinol in other model.
- Study the effect of silanization of Nitinol with crosslinking agents.

Though the present study focused on in-vitro and in-vivo performance of bare, silanized and coated nitinol samples few more steps are immediately needed to make the work more comprehensive in nature. It is a known fact that surface modification is inevitable for nitinol to avoid nickel release. However all the probable options for such modifications could not be tried in the present study. We propose to conduct a more elaborate and systematic study both on biological surface modification and inorganic coating development in future.

As far as in-vivo and in-vitro studies are concerned we have done mostly the standard tests including micro-CT to get meaningful data. The results obtained in the present study revealed that there was no particular variety of nitinol which was better in all aspects. In future we should go for more elaborate study (if possible involving other animal models) with lot of other parameters to get a meaningful comparison.

Betterment of coating ensuring good adhesion and modification of silanization with crosslinking are the two other prospective domains where the present work can be further extended.

At the end , it is envisaged that the study can be extended further following a systematic path to develop nitinol implants particularly in the form of kink resistant orthopaedic nail or pin.